Spin-Lattice Relaxation of Rare-Earth Ions in LaF_3†

M. B. SCHULZ AND C. D. JEFFRIES*
Department of Physics, University of California, Berkeley, California
(Received 3 February 1966; revised manuscript received 19 May 1966)

The spin-bath relaxation rate T_b^{-1} has been measured in the temperature range $1.3 < T < 5$°K for each of the trivalent Kramers ions: Ce^{3+}, Nd^{3+}, Sm^{3+}, Gd^{3+}, Dy^{3+}, Er^{3+}, and Yb^{3+}, magnetically diluted in LaF_3. In three cases, Nd^{3+}, Er^{3+}, and Yb^{3+}, the temperature range was extended to $0.2 < T < 5$°K. All measurements were made by observing the transient recovery of the microwave paramagnetic resonance at the frequency $\nu \approx 9.3$ Gc/sec. The temperature dependence of the Orbach process $T_{1O}^{-1} \propto \exp(-\Delta/T)$ is displayed for Nd, Sm, and Er; and the Raman process $T_{1R}^{-1} \propto T^9$ is displayed for Nd, Er, and Yb. These do not depend on crystal orientation nor on the concentration of paramagnetic ions. The values $\Delta(\mathrm{Nd}) = 57$°K and $\Delta(\mathrm{Er}) = 72$°K are found to agree reasonably with the energy of the first crystal-field state, previously determined optically; we find $\Delta(\mathrm{Sm}) = 50$°K. The direct process, $T_{1d}^{-1} \propto T$, is observed only for the lowest concentrations of paramagnetic ions: 0.1% Nd and 0.05% Er. For other ions and at higher concentrations the direct process was usually obscured by cross relaxation, probably to excited states of exchange coupled pairs or larger clusters of magnetic ions as evidenced by a temperature dependence $T_b^{-1} \propto \mathrm{csch}(\Delta'/kT)$, where Δ' is of order of the exchange energy. No clear-cut example of a phonon bottleneck, $T_b^{-1} \propto T^2$, is found. From optical data for Nd and Er, wave functions and crystal-field parameters are obtained, from which simple theoretical estimates of the relaxation rates are found to be in moderate agreement with the data.

I. INTRODUCTION

BECAUSE of the close relationship to nuclear relaxation and dynamic nuclear orientation, maser and laser operation, microwave phonon experiments, etc., there has been interest lately in measuring the spin-lattice relaxation rate at low temperatures of paramagnetic rare-earth ions, especially when diluted into various diamagnetic host crystals.[1–20] The basic relaxation mechanism appears to be that of Van Vleck[21] and Kronig,[22] in which the ion interacts with the thermally-modulated crystalline electric fields. The phenomenological formulation of Orbach[23] can give order-of-magnitude estimates of the relaxation rate; such estimates agree reasonably well with the relaxation data in those cases where the paramagnetic ions fit into crystal lattice sites which are well separated from each other, e.g., lanthanum magnesium nitrate, lanthanum ethyl sulfate, yttrium ethyl sulfate.[1–3,18] However, the crystal-field theory cannot account for a strong dependence of the observed relaxation rate at low temperatures on the concentration of the paramagnetic ion in crystals such as CaF_2,[12] LaF_3,[14,24] and several garnets.[9,17] This concentration dependence is generally felt to be due to cross relaxation[25,26] to exchange coupled pairs or larger clusters of paramagnetic ions, and may mask the true spin-lattice (i.e., spin-phonon) relaxation rate T_1^{-1} due to the Van Vleck–Kronig mechanism. Actually, in the present experiments, as in most other relaxation measurements, what is observed is the total spin-bath relaxation rate T_b^{-1} between the paramagnetic ion in question and the helium bath in which the crystal is immersed. Thus T_b^{-1} is determined by cross relaxation effects and phonon bottlenecking[2] as well as T_1^{-1}.

By observing the transient recovery of the microwave paramagnetic resonance absorption following a saturating pulse, we have measured the spin-bath relaxation rate in the temperature range $1.3 < T < 5$°K for the ions Ce^{3+}, Nd^{3+}, Sm^{3+}, Gd^{3+}, Dy^{3+}, Er^{3+}, and Yb^{3+} diluted into LaF_3 in various concentrations from 0.05 to 1.5%.

† Supported in part by the U. S. Atomic Energy Commission.
* NSF Fellow, 1965–1966, in Division of Applied Physics, Pierce Hall, Harvard University, Cambridge, Massachusetts.

[1] C. B. P. Finn, R. Orbach, and W. P. Wolf, Proc. Phys. Soc. (London) **A77**, 261 (1961).
[2] P. L. Scott and C. D. Jeffries, Phys. Rev. **127**, 32 (1962).
[3] R. H. Ruby, H. Benoit, and C. D. Jeffries, Phys. Rev. **127**, 51 (1962).
[4] J. A. Cowen, D. E. Kaplan, and M. E. Browne, J. Phys. Soc. Japan **17**, Suppl. B-I, 465 (1962).
[5] G. M. Zverev, L. S. Kornienko, A. N. Prokhorov, and A. I. Smirnov, Fiz. Tverd. Tela **4**, 392 (1962)[English transl.: Soviet Phys.—Solid State **4**, 284 (1962)].
[6] J. Van den Broek and L. C. Van der Marel, Physica **29**, 948 (1963).
[7] J. C. Gill, Proc. Phys. Soc. (London) **82**, 1066 (1963).
[8] G. Weber, Z. Physik **171**, 335 (1963).
[9] I. Svare and G. Seidel, in *Proceedings of the First International Conference on Paramagnetic Resonance, Jerusalem, 1962*, edited by W. Low (Academic Press Inc., New York, 1963), Vol. II, p. 430.
[11] P. P. Pashinin and A. M. Prokhorov, Fiz. Tverd. Tela **5**, 359 (1963) [English transl.: Soviet Phys.—Solid State **5**, 261 (1963)].
[12] M. J. Weber and R. W. Bierig, Phys. Rev. **134**, A1492 (1964); R. W. Bierig, M. J. Weber, and S. I. Warshaw, *ibid.* **134**, A1504 (1964).
[13] H. Kalbfleisch, Z. Physik **181**, 13 (1964).
[14] J. M. Baker and N. C. Ford Jr., Phys. Rev. **136**, A1692 (1964).
[15] N. E. Kask, L. S. Kornienko, A. N. Prokhorov, and M. Fakir, Fiz. Tverd. Tela **5**, 2303 (1963); **6**, 549 (1964) [English transls.: Soviet Phys.—Solid State **5**, 1675 (1964); **6**, 430 (1964)].
[16] D. J. Griffiths, thesis, University of British Columbia, 1965 (unpublished).
[17] C. Y. Huang, Phys. Rev. **139**, A241 (1965).
[18] G. H. Larson and C. D. Jeffries, Phys. Rev. **141**, 461 (1966); **145**, 311 (1966).
[19] R. C. Mikkelson and H. J. Stapleton, Phys. Rev. **140**, A1968 (1965).
[20] B. W. Mangum and R. P. Hudson (unpublished).
[21] J. H. Van Vleck, Phys. Rev. **57**, 426 (1940).
[22] R. de L. Kronig, Physica **6**, 33 (1939).
[23] R. Orbach, Proc. Roy. Soc. (London) **A264**, 456 (1961).
[24] M. B. Schulz and C. D. Jeffries, Bull. Am. Phys. Soc. **9**, 739 (1964).
[25] N. Bloembergen, S. Shapiro, P. S. Pershan, and J. O. Artman, Phys. Rev. **114**, 445 (1959).
[26] A. Rannestad and P. E. Wagner, Phys. Rev. **131**, 1953 (1963).

In three cases, Nd^{3+}, Er^{3+}, and Yb^{3+}, the temperature range was extended to $0.2<T<5°K$. Some of this work has been briefly reported earlier.[24] In a sense this work is an extension of that of Scott and Jeffries[2] to which we frequently refer as S&J.

II. THE CRYSTAL STRUCTURE OF LaF_3 AND PARAMAGNETIC RESONANCE

The first x-ray investigation of LaF_3 was performed by Oftedal[27] who suggested that LaF_3 is hexagonal with a unit cell containing six molecules. Later Schlyter,[28] proposed a smaller unit cell containing only two molecules. Caspers *et al.*[29] have studied the lattice vibrations of LaF_3. Comparison of predicted modes of vibration from group theory for the two types of unit cells with their data seems to favor the smaller unit cell. On the other hand, electron paramagnetic resonance (EPR) studies[30,31] indicate that there are six magnetically inequivalent sites for paramagnetic rare-earth ions magnetically diluted into LaF_3 with a site symmetry of C_{2h} or lower. Optical-absorption and fluorescence studies[32–34] on doped samples seem to disagree with the EPR work, since partially polarized spectra are observed, suggesting a higher site symmetry.

From studies of the perturbation of the nuclear magnetic resonance of La^{139} by the interaction between the electric quadrupole moment and the crystalline electric field gradient, Andersson and Proctor[35] find six inequivalent La sites and conclude that there are six molecules per unit cell and that the La site symmetry is C_s. Recent x-ray structure redeterminations[36,37] by Mansmann and by Zalkin *et al.* arrive at the structure of Fig. 1, with six molecules per unit cell and C_2 point symmetry about the La site; each La has six La neighbors at 4.23 Å. They conclude that the crystals are trigonal rather than hexagonal, and that there should be only three inequivalent La sites. This discrepancy between the x-ray data and the EPR and NMR data has not yet been resolved. Possibly there is a phase transition or possibly the crystals used in the magnetic resonance studies have been twinned.

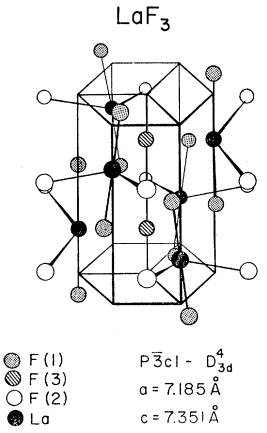

FIG. 1. The structure for the 6-molecule unit cell of LaF_3, (Ref. 36). The hexagonal prism has volume $\frac{1}{3}$ that of the unit cell.

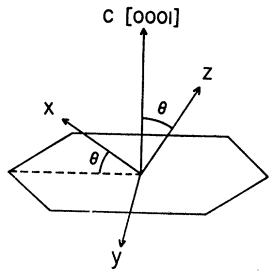

FIG. 2. The orientation of the principal axes (x,y,z) of the g tensor for rare-earth ions in LaF_3. The value of θ for each ion is given in Table I.

Neglecting hyperfine structure, the magnetic-resonance results of Baker and Rubins[31] on doped samples can be described by the effective spin Hamiltonian for Kramers doublets

$$\mathcal{H}=\beta(g_xH_xS_x+g_yH_yS_y+g_zH_zS_z), \qquad (1)$$

where g_x, g_y, and g_z are the principal values of the g tensor, and the effective spin $S=\frac{1}{2}$. Gd^{3+} in LaF_3 is described by[30]

$$\mathcal{H}=g\beta\mathbf{H}\cdot\mathbf{S}+\sum_{\substack{n=2,4,6\\ m=0,2,4,6}} B_n{}^mO_n{}^m. \qquad (2)$$

There are six magnetically inequivalent lanthanum sites into which a paramagnetic ion may substitute and each of these six sites is described by an identical Hamiltonian, the only difference being in the orientation of the principal axes (x,y,z) of the g tensor. These are derived from one another by 120° rotations about the crystal c axis and reflection in the plane perpendicular to it. The y axis lies in the plane perpendicular to the c axis and is perpendicular to one of the cleavage planes; see Fig. 2. The angle θ, which is the angle between the z axis of the g tensor and the crystal c axis is found to be different for each rare earth ion. Since the ionic radii of the trivalent rare earths contract by approximately 20% in going through the rare-earth series[38] from La^{3+} to Lu^{3+} it is easy to see that the lattice might distort somewhat when another ion is substituted for La^{3+}. In fact Zalkin and Templeton[39] find that concentrated

[27] I. Oftedal, Z. Physik. Chem. **B5**, 272 (1929); **B13**, 190 (1931).
[28] K. Schlyter, Arkiv Kemi **5**, 73 (1952).
[29] H. H. Caspers, R. A. Buchanan, and H. R. Marlin, J. Chem. Phys. **41**, 94 (1964).
[30] D. A. Jones, J. M. Baker, and D. F. D. Pope, Proc. Phys. Soc. (London) **74**, 249 (1959).
[31] J. M. Baker and R. S. Rubins, Proc. Phys. Soc. (London) **78**, 1353 (1961).
[32] E. Wong, O. Stafsudd, and D. Johnston, J. Chem. Phys. **39**, 786 (1963).
[33] E. Wong, O. Stafsudd, and D. Johnston, Phys. Rev. **131**, 990 (1963).
[34] W. F. Krupke and J. B. Gruber, J. Chem. Phys. **39**, 1024 (1963).
[35] L. O. Andersson and W. G. Proctor, Z. Krist (to be published).
[36] Von M. Mansmann, Z. Anorg. Allgem. Chem. **331**, 98 (1964).
[37] A. Zalkin, D. H. Templeton, and T. E. Hopkins (unpublished).
[38] D. H. Templeton and C. H. Dauben, J. Am. Chem. Soc. **76**, 5237 (1954).
[39] A. Zalkin and D. H. Templeton, J. Am. Chem. Soc. **75**, 2453 (1953).

TABLE I. Resonance results for rare-earth ions in LaF_3.

Ion	Temperature (°K)	g_x	g_y	g_z	θ (deg)	Ref.
$La^{3+}(4f^0)$	300				53.4±0.5	35
$Ce^{3+}(4f^1)$	20	0.32 ±0.01	0.90 ±0.02	2.608±0.005	14 ±1	31
$Nd^{3+}(4f^3)$	4.2	1.356±0.006	1.092±0.005	3.11 ±0.03	45 ±2	31
$Sm^{3+}(4f^5)$	4.2	0.23 ±0.01	0.558±0.005	0.720±0.007	14.5±0.2	this paper
$Gd^{3+}(4f^7)$	90		($g_x=g_y=g_z$	=1.990±0.001)	0	30
$Dy^{3+}(4f^9)$	4.2	5.52 ±0.05	0.96 ±0.01	13.8 ±0.2	16 ±2	this paper
$Er^{3+}(4f^{11})$	20	2.99 ±0.05	4.91 ±0.04	10.89 ±0.05	44 ±1	31
	14	2.98 ±0.03	4.91 ±0.03	11.09 ±0.04	45 ±½	
$Yb^{3+}(4f^{13})$	20	3.76 ±0.03	5.20 ±0.01	1.210±0.005	10 ±3	31

rare-earth trifluorides do not all have the same crystal structure.

Table I lists the values of the g tensor and θ as determined by paramagnetic resonance by Baker and Rubins[31] and also by our measurements. The value of θ listed for La^{3+} is taken from Andersson and Proctor[35] and determines the orientation of the nuclear quadrupole tensor. The spin Hamiltonian parameters[30] for Gd^{3+} are listed in Table II. The linewidth of the paramagnetic resonance is typically 20 to 50 Oe and is independent of concentration below 1%. This width is much greater than the Van Vleck dipolar linewidth, and is probably due to unresolved hfs with the F ions surrounding the paramagnetic ion, as discussed later.

The samples used in our experiments were obtained from Varian Associates and were grown by Hugh Muir in a HF atmosphere using a Bridgman technique.[40] Some of the samples showed cleavage planes, (0001), although they did not have the metallic reflection property described by Baker and Rubins[31] for the (0001) planes of their samples. This difference is probably due to a different annealing technique. We usually oriented our samples by studying the Lauè pattern of x rays scattered from the surface of the crystal.

In Fig. 3 we show a typical paramagnetic resonance spectrum, that for a sample of LaF_3 containing 0.1% Nd^{3+}. This clearly shows six strong lines due to six magnetically inequivalent sites. The weaker incompletely resolved lines are due to hyperfine interaction $\mathbf{I}\cdot\mathbf{A}\cdot\mathbf{S}$ with Nd^{143} and Nd^{145} nuclei, each having nuclear spin $\frac{7}{2}$ and natural abundance 12.2 and 8.3%, respectively.

TABLE II. Spin-Hamiltonian parameters for Gd^{3+} in CaF_3 at 90°K from Ref. 30. The units are 10^{-4} cm^{-1}.

$$b_2^0=3B_2^0=+239\pm1$$
$$b_2^2=3B_2^2=-5\pm2$$
$$b_4^0=60B_4^0=+5.6\pm0.2$$
$$b_4^2=60B_4^2=+27\pm3$$
$$b_4^4=60B_4^4=-43\pm3$$
$$b_6^0=1260B_6^0=-0.14\pm0.2$$
$$b_6^2+b_6^6=1260(B_6^2+B_6^6)=+8.5\pm3$$
$$b_6^4=1260B_6^4=-1\pm5$$
$$g=1.990\pm0.001$$

Because of the low symmetry of the crystalline field at the lanthanum site, it is expected that all degeneracy will be lifted for ions containing an even number of electrons and hence not subject to Kramers' theorem. The splitting may be considerably larger than a microwave quantum[41]; this is probably why we failed to observe paramagnetic resonance in LaF_3 crystals doped with Pr^{3+} and with Tb^{3+}. In fact no paramagnetic resonance has ever been reported for non-Kramers ions in LaF_3.

III. REVIEW OF RELAXATION THEORY

A proper approach to spin-lattice relaxation would be, following Van Vleck,[21] to analyze the normal modes of vibration of the crystal in question. Orbach[23] has noted, however, that the rare-earth ions can be handled in a simple phenomenological treatment because the crystal-field interaction is much weaker than the spin-orbit interaction and therefore leaves $\mathbf{J}=\mathbf{L}+\mathbf{S}$ a good quantum number. We consider just the ground elec-

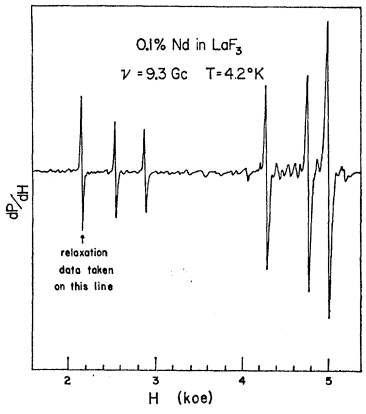

FIG. 3. The derivative dP/dH of the paramagnetic-resonance spectrum of Nd^{3+} in LaF_3. The crystal is oriented with the external dc field $H\|z$ for the site whose main line is at 2120 Oe.

[40] P. W. Bridgman, Proc. Am. Acad. Arts Sci. 60, 305 (1925).

[41] H. H. Caspers, H. E. Rast, and R. A. Buchanan, J. Chem. Phys. 43, 2124 (1965).

tronic state, which can be described by the Hamiltonian

$$\mathcal{H}=\mathcal{H}_{so}+\mathcal{H}_c+\mathcal{H}_z, \tag{3}$$

where the terms represent the spin-orbit, crystal field, and Zeeman interactions, respectively. For LaF_3 with C_2 or C_s symmetry the crystal-field interaction is given by

$$\mathcal{H}_c=\sum_{\substack{n=2,4,6\\ m=0,\pm2,\pm4,\pm6}} A_n{}^m G_n{}^m(x,y,z), \tag{4}$$

where $G_n{}^m$ is an unnormalized tesseral harmonic and $A_n{}^m$ is a crystal-field parameter. The effect of each term in Eq. (3) is represented in Fig. 4 for the case of an ion having an odd number of electrons. For our experiments the Zeeman splitting $\delta=h\nu\approx0.3$ cm^{-1}.

Our experiments consist in placing a single crystal in a microwave cavity immersed in a liquid-helium bath at temperature T and in a dc magnetic field H. Electron spin resonance is observed only between the states of the lowest doublet $|a\rangle$ and $|b\rangle$ since only they are significantly populated at helium temperature. We are concerned with the rate $T_1{}^{-1}$ at which the population difference N_a-N_b returns to its thermal equilibrium value after a saturating microwave pulse of energy $\delta=h\nu$. We assume that the ion is coupled to the lattice by a phenomenological Hamiltonian $\mathcal{H}_c'$, which couples the fluctuating crystal field to the orbital angular momentum and acts as a random time dependent perturbation to induce spin transitions between $|b\rangle$ and $|a\rangle$. Now $\mathcal{H}_c'$ is obtained, approximately,[23,2] by expanding the static crystal-field term, Eq. (4). We assume that $A_n{}^m(\xi)$ depends on a ligand coordinate ξ and expand $A_n{}^m(\xi)$ in a Taylor series:

$$A_n{}^m(\xi)=A_n{}^m(\xi)_0+\epsilon\xi\left(\frac{\partial A_n{}^m}{\partial\xi}\right)_0 +\tfrac{1}{2}\epsilon\epsilon'\xi\xi'\left(\frac{\partial^2 A_n{}^m}{\partial\xi\partial\xi'}\right)_0+\cdots, \tag{5}$$

where ϵ is the thermal lattice strain. The first term is just the static crystal-field term, usually known experimentally from optical data. The second term can be evaluated by using a simple point-charge model for which $A_n{}^m(\xi)\propto\xi^{-(n+1)}$ yielding for the relaxation Hamiltonian

$$\mathcal{H}_c'=\epsilon\sum v_n{}^m=\epsilon\sum a_n{}^m G_n{}^m(x,y,z), \tag{6}$$

where the dynamic parameters $a_n{}^m$ are related to the static parameters by

$$|a_n{}^m|\approx|\xi(\partial A_n{}^m/\partial\xi)_0|\approx(n+1)|A_n{}^m|. \tag{7}$$

Although the factor $(n+1)$ was neglected in the earlier approximations[23,2] it has been included more recently[17,18] and we will find in Sec. V that better agreement obtains for LaF_3 if we include it. The matrix elements of $v_n{}^m$ can be evaluated by the operator equivalent method

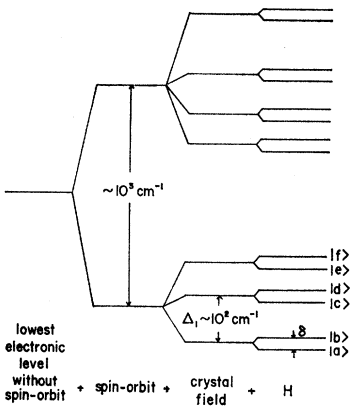

FIG. 4. Effect of each term in Eq. (3) on the electronic ground state of a hypothetical rare-earth ion with Kramers degeneracy doped into a diamagnetic crystal.

of Stevens.[42] There are at least three distinct processes, adequately discussed previously[21,23,2]: the direct, the Orbach, and the Raman.

Direct process. In this processes a spin flip from $|b\rangle$ to $|a\rangle$ occurs simultaneously with the creation of a phonon of energy $\delta=h\nu$. From Eq. (6) and first-order time-dependent perturbation theory the over-all result for the direct relaxation rate for a Kramers salt is found to be

$$\frac{1}{T_{1d}}=\frac{3}{2\pi\rho v^5\hbar}\left(\frac{\delta}{\hbar}\right)^3\sum_{n,m}\Big|\sum_i\left(\frac{2\beta\Lambda}{\Delta_i}\right)(\langle a|\mathbf{H}\cdot\mathbf{J}|i\rangle\langle i|v_n{}^m|b\rangle +\langle a|v_n{}^m|i\rangle\langle i|\mathbf{H}\cdot\mathbf{J}|b\rangle)\Big|^2\coth\left(\frac{\delta}{2kT}\right), \tag{8}$$

where ρ is the crystal density, v is a suitably averaged velocity of sound, β is the Bohr magneton, Λ is the Landé g factor, $|i\rangle$ is one of the states for each higher Kramers doublet at Δ_i and the sum $\sum_i$ is over all the excited doublets, $\mathbf{H}$ is the dc field. For $\delta\ll kT$, $\coth(\delta/2kT)\approx(2kT/\delta)$, yielding the familiar form for the temperature and field dependence of the direct process

$$1/T_{1d}=KH^4T. \tag{9}$$

This process should display no dependence on crystal size or paramagnetic concentration for dilute samples. Equation (8) is identical to Eq. (18) of S&J except for the summation over excited states and the factor $(n+1)$ implicitly contained in $v_n{}^m$. Although the relationship of Eq. (7) is only an order of magnitude approximation, it is probably a better approximation to include the factor $(n+1)$.

Orbach process. In cases where the Debye temperature Θ_D is higher than the splitting, Δ_1/k, between the two lowest doublets, relaxation may take place via the two-step Orbach process.[1,23] For LaF_3, $\Theta_D=360$°K.[43]

[42] K. W. H. Stevens, Proc. Phys. Soc. (London) **A65**, 209 (1952).
[43] W. M. Yen, W. C. Scott, and A. L. Schawlow, Phys. Rev. **136**, A271 (1964).

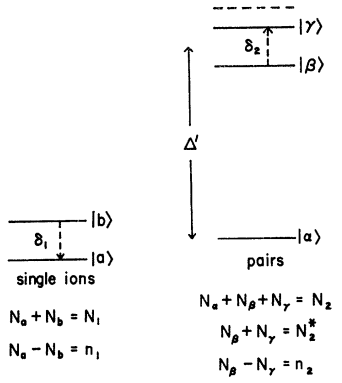

FIG. 5. Energy levels $|a\rangle$ and $|b\rangle$ of a single ion, and levels $|\alpha\rangle$, $|\beta\rangle$, and $|\gamma\rangle$ of a pair of ions.

Under the reasonable assumption, $\delta \ll \Delta_1$, the relaxation rate for a Kramers doublet due to the Orbach process is

$$\frac{1}{T_{10}} \approx \frac{12}{2\pi\rho v^5 \hbar}\left(\frac{\Delta_1}{\hbar}\right)^3 \frac{\sum_{n,m} |\langle a|v_n^m|c\rangle|^2 \sum_{n,m} |\langle c|v_n^m|b\rangle|^2}{\sum_{n,m} |\langle a|v_n^m|c\rangle|^2 + \sum_{n,m} |\langle c|v_n^m|b\rangle|^2} \times [\exp(\Delta_1/KT)-1]^{-1}. \quad (10a)$$

For $\Delta_1 \gg kT$, this takes the form

$$1/T_{10} \approx B \exp(-\Delta_1/kT). \quad (10b)$$

Raman Process. This process involves the simultaneous absorption of a phonon of energy δ_1 and the emission of another of energy $\delta_2 = \delta_1 + \delta$, along with a spin flip from $|b\rangle$ to $|a\rangle$. It is of higher order than the Orbach process in the sense that it arises in second order time dependent perturbation theory using $\mathcal{H}_c'$ of Eq. (6), and also in first-order time-dependent theory from the perturbation $\epsilon_1\epsilon_2 \sum v_n^m$ from the third term of Eq. (5). For Kramers salts, usually the former dominates, the overall result being

$$\frac{1}{T_{1R}} = \frac{9!\hbar^2}{\pi^3\rho^2 v^{10}}\left(\frac{k}{\hbar}\right)^9 \sum_i \Delta_i^{-4} \sum_{n,m} |\langle a|v_n^m|i\rangle|^2 \times \sum_{n,m} |\langle i|v_n^m|b\rangle|^2 T^9 \equiv CT^9. \quad (11)$$

Summarizing the foregoing, one finds generally for Kramers ions that

$$1/T_1 = AT + B\exp(-\Delta_1/kT) + CT^9. \quad (12)$$

Equations (8), (10), and (11) are the equations we use in Sec. V to estimate the relaxation rates. For the calculation of the various matrix elements in these equations, we refer to S&J Eqs. (15) and (16):

$$\sum_{n,m} |\langle a|v_n^m|c\rangle|^2 = \sum_{\substack{n=2,4,6 \\ -n \leq m \leq n}} |\chi_n a_n^m \langle r^n\rangle \langle a|o_n^m|c\rangle|^2, \quad (13)$$

where the χ_n are operator equivalent factors equal to the α, β, and γ of Stevens.[42] We note that whereas the static field interaction, Eq. (4) contains only certain terms $m=0, \pm 2, \pm 4, \pm 6$ because of symmetry, we assume that all dynamic terms may exist in (13), and furthermore assume that the a_n^m and a_n^{-m} terms are incoherent. The terms $a_n^m\langle r^n\rangle$ are the dynamic crystalline field parameters in an expansion in unormalized tesseral harmonics. As discussed in Sec. V these are estimated in various ways, usually from the known static field parameters $A_n^m\langle r^n\rangle$. The operators o_n^m are defined by $o_n^m + o_n^{-m} = O_n^m$, which are operators in $J_\pm$, J_z and have been tabulated.[23,44]

Phonon bottleneck. It is well to discuss here several assumptions leading to Eqs. (8), (10), and (11). First, a continuous Debye spectrum is assumed, i.e., a density of phonon states $\propto \delta^2$. Also the phonon excitation number is assumed to have its thermal equilibrium value $p = p_0 = [\exp(\delta/kT)-1]^{-1}$. However, if the rate of energy transfer from the spins to the crystal phonons significantly exceeds the transfer rate from phonons to helium bath, then a "phonon bottleneck"[45] may develop. This has been observed and analyzed in detail in S&J in other rare-earth salts. The over-all result is that one observes a spin-bath relaxation rate

$$\frac{1}{T_b} \approx \frac{12\pi\nu^2\Delta\nu}{T_{ph}v^3c}\coth^2\left(\frac{h\nu}{2kT}\right) \approx DT^2, \quad (14)$$

where $\Delta\nu$ is the spin-resonance linewidth, T_{ph} is the phonon-bath relaxation time, c is the number of paramagnetic ions per cc, and v the velocity of sound. This bottleneck process is observed in lieu of the direct process, and is distinguished from it by its different temperature dependence, a concentration dependence, and possibly a sample size dependence through T_{ph}.

Cross relaxation.[25,26,46] Up until now we have been assuming that the spins relax directly to the lattice phonons and thence to the helium bath. In LaF_3 the situation may be much more complicated, in contrast to softer crystals, e.g., the double nitrates and the ethyl sulfates.[2,3,18] In these soft crystals the velocity of sound is low ($v \approx 2\times10^5$ cm/sec) and the direct relaxation process is fairly strong, since $T_{1d} \propto v^5$. Also the closest La-La spacing is ~ 8 Å, and magnetic interaction between pairs of ions is purely dipolar, i.e., fairly weak, and the paramagnetic resonance lines are correspondingly sharp. Thus even at concentrations of a few percent the true direct process dominates over cross relaxation to pairs of magnetic ions. On the other hand in LaF_3, the velocity of sound is greater, $v_l \approx 6\times10^5$ cm/sec and $v_t \approx 2.3\times10^5$ cm/sec, making the direct process weaker; furthermore the nearest La-La spacing is 4.2 Å, and

[44] M. T. Hutchings, in *Solid State Physics*, edited by F. Seitz and D. Turnbull (Academic Press Inc., New York, 1965), Vol. 16, p. 227.

[45] J. H. Van Vleck, Phys. Rev. **59**, 724 (1941).

[46] N. Bloembergen, P. S. Pershan, J. H. Van Vleck, J. C. Gill, and R. J. Elliot, in *Advances in Quantum Electronics*, edited by J. R. Singer (Columbia University Press, New York, 1961), pp. 373–403.

there is considerable interaction between magnetic neighbors. In fact, the paramagnetic resonance linewidth of 20 to 50 Oe is due to hfs interaction with the F neighbors at 2.4 Å. Thus at the lowest temperatures the direct process can easily be dominated by cross relaxation effects to pairs of magnetic ions, which themselves relax rapidly to the lattice. Anticipating the experimental results in Sec. V that at the lowest temperatures the observed relaxation rates are concentration dependent and are one or two orders of magnitude stronger than theoretical estimates of the direct process, we briefly review the pertinent model of cross relaxation.[26,46,47]

We assume a uniform spatial distribution throughout the crystal of a total of N_1 single paramagnetic ions in a ground state Kramers doublet $|a\rangle$ and $|b\rangle$, as shown in Fig. 5, and a total of N_2 pairs of these ions randomly distributed, and having an antiferromagnetic singlet ground state $|\alpha\rangle$ and an excited triplet state, two levels of which we denote by $|\beta\rangle$ and $|\gamma\rangle$, at energy Δ', which we refer to as an "excited doublet." If $\delta_1 \approx \delta_2$, then the ith single ion can flip from $|b\rangle$ to $|a\rangle$ simultaneously with the jth pair flipping from $|\beta\rangle$ to $|\gamma\rangle$ with a reasonable probability w_{ij}. The rate equation for this cross relaxation process is

$$\dot{n}_1 = w(-N_2^* n_1 + N_1 n_2) = -\dot{n}_2 , \tag{15}$$

where n_1 is the population difference of the single ion doublet, n_2 is the population difference of the excited pair doublet, N_2^* is the total population of the excited pair doublet, and

$$w = \frac{1}{N_1} \sum_{i=1}^{N_1} w_{ij} , \tag{16}$$

Eq. (15) has as its time constant, the cross relaxation time

$$T_{21} = [w(N_1 + N_2^*)]^{-1} . \tag{17}$$

We are only interested in the case $N_2^* \ll N_1$, for which

$$T_{21}^{-1} \approx \sum_{i=1}^{N_1} w_{ij} \approx C_1 \Delta\omega , \tag{18}$$

where C_1 is the fractional concentration of single paramagnetic ions in the diamagnetic host, and $\Delta\omega$ is of the order of the Van Vleck linewidth for a hypothetical magnetically concentrated crystal, calculated from the usual lattice dipolar sums. If δ_1 is not exactly equal to δ_2, Eq. (18) must be further reduced by a proper line shape factor; however the exact magnitude of T_{21}^{-1} is not crucial to the following discussion. We further assume that the single ions have a spin-lattice relaxation time T_1 and the excited doublet a spin-lattice relaxation time T_1^*, so that the total rate equations

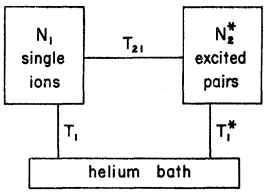

FIG. 6. Thermal block diagram of the system of Fig. 5.

become

$$\dot{n}_1 = w(-N_2^* n_1 + N_1 n_2) - \frac{n_1 - n_{10}}{T_1} , \tag{19a}$$

$$\dot{n}_2 = w(-N_1 n_2 + N_2^* n_1) - \frac{n_2 - n_{20}}{T_1^*} . \tag{19b}$$

For $N_2^* \ll N_1$ these coupled rate equations can be solved[26] and it is shown that, following saturation of n_1, the population difference of the single ions and hence the signal recovers principally at the rate λ^-, where

$$\lambda^- \approx \frac{1}{T_1} + \left[\frac{1}{T_{21}}\left(\frac{1}{T_1^*} - \frac{1}{T_1}\right) \Big/ \left(\frac{1}{T_{21}} + \frac{1}{T_1^*} - \frac{1}{T_1}\right)\right]\left(\frac{N_2^*}{N_1}\right) . \tag{20}$$

As can be seen from the thermal block diagram of Fig. 6, there are several approximate forms which Eq. (20) may take, depending on the relative magnitudes of T_{21}, T_1, and T_1^*. The simplest and almost trivial case is

$$\frac{1}{T_1} \gg \frac{1}{T_{21}} \quad \text{and} \quad \frac{1}{T_1^*} ; \quad \lambda^- \approx \frac{1}{T_1} . \tag{21a}$$

As expected, the observed rate is simply the spin lattice relaxation rate of the single ions. Another case is

$$\frac{1}{T_{21}} \gg \frac{1}{T_1^*} \gg \frac{N_1}{N_2^*}\frac{1}{T_1} ; \quad \lambda^- \approx \frac{N_2^*}{N_1}\frac{1}{T_1^*} . \tag{21b}$$

This is the case of strong cross relaxation and weak spin lattice relaxation of the single ions; one observes a relaxation rate for the single ions equal to the spin-lattice rate T_1^{*-1} of the excited pairs, reduced by the factor N_2^*/N_1, which is just the specific heat ratio of the two systems. Another simple case is

$$\frac{1}{T_1^*} \gg \frac{1}{T_{21}} \gg \frac{N_1}{N_2^*}\frac{1}{T_1} ; \quad \lambda^- \approx \frac{N_2^*}{N_1}\frac{1}{T_{21}} . \tag{21c}$$

This is the case for very strong spin-lattice relaxation of the excited pair; the observed rate is the cross relaxation rate T_{21}^{-1}, reduced by the factor N_2^*/N_1.

Equation (21b) can be evaluated for the system of Fig. 6, where $N_1 \propto C_1$, $N_2 \propto C_1^2$, $N_2^* \propto C_1^2[1+\exp(\Delta'/kT)]^{-1}$, and $T_1^{*-1} \propto \Delta'^3[1-\exp(-\Delta'/kT)]^{-1}$, as can be shown for an "inverse" Orbach process for the ex-

[47] J. C. Gill, Proc. Phys. Soc. (London) **79**, 58 (1962).

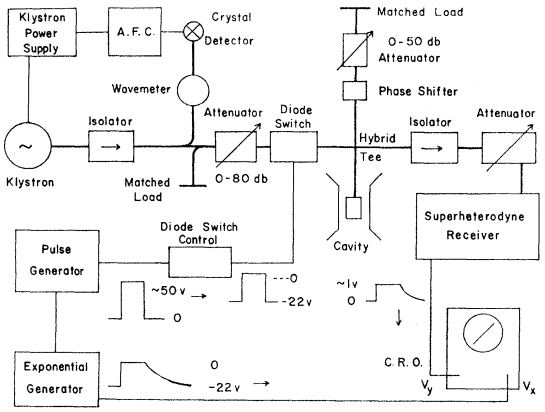

FIG. 7. Block diagram of paramagnetic-resonance spectrometer used for measuring relaxation rates at 9.3 Gc/sec.

cited doublet, if $\Delta' \gg kT$. This yields

$$\lambda^- \propto C_1 \Delta'^3 \operatorname{csch}(\Delta'/kT), \tag{22}$$

for the expected temperature and concentration dependence for strong cross relaxation. If $\Delta' \gg kT$, this becomes approximately $\lambda^- \propto C_1 \Delta'^3 \exp(-\Delta'/kT)$, showing a temperature dependence which turns out to have the same form as an ordinary Orbach process.

Equation (21c) can be evaluated to yield

$$\lambda^- \propto C_1^2[1+\exp(\Delta'/kT)]^{-1}, \tag{23}$$

for the case of strong lattice relaxation of the excited pair, which also shows the same temperature dependence as an Orbach process in the limit $\Delta' \gg kT$, but with a quadratic concentration dependence.

The true situation is apt to be more complicated because there may be a variety of pairs or clusters with a distribution of values of Δ'. For example, Gill[47] finds that a suitably averaged value of Eq. (22) for Cr^{3+} in Al_2O_3 can yield an approximate temperature dependence $\lambda^- \propto T^2$, which has the same form as a phonon bottleneck.

Rather than cross relaxation to pairs, it is also possible to have cross relaxation from the observed Kramers doublet $|a\rangle$ and $|b\rangle$ of Fig. 6 to the ground state Kramers doublet of an impurity magnetic ion of concentration C' and spin-lattice relaxation rate T_1'. In this case Eq. (21b) leads to an observed relaxation rate $\lambda^- \approx (C'/C_1)T_1'^{-1}$, showing the temperature dependence of the impurity ion. Similarly Eq. (21c) leads to $\lambda^- \propto C'$, independent of temperature.

We summarize this review by remarking that cross relaxation can evidently lead to a wide variety of concentration and temperature dependences, and that such effects will be more readily observed at low temperatures in LaF_3 crystals than in the softer hydrated crystals, where the true direct process is stronger and cross relaxation weaker.

IV. EXPERIMENTAL APPARATUS AND PROCEDURES

All of our measurements of the spin-bath relaxation time T_b were made at a fixed frequency $\nu \approx 9.3$ Gc/sec, using the pulse-saturation-recovery technique. Four different spectrometers were used: the one shown in Fig. 7; the one described in S&J, Fig. 2; the one described in Ruby *et al.*,[3] Figs. 1 and 2; and the one described by Larson and Jeffries I,[18] Fig. 4. The diode microwave switch, Fig. 7, a Philco Mount P901A with L4146 germainum diode, could be tuned to give an on-off ratio of approximately 30 dB. The spin-bath relaxation time was observed by operating the klystron at some fixed power level and frequency and the dc magnetic field at the resonant value; pulsing the diode switch allowing it to pass pulses of microwave power to the sample, thus saturating the spin levels; and then observing, at low monitoring level, the recovery of the resonance signal to its thermal equilibrium value. Usually a fast initial recovery was observed due to recovery of the receiver ($\approx 10^{-6}$ sec), as well as possible cross relaxation effects within the resonance linewidth. The initial fast recovery was usually followed by an exponentially recovering signal. The pulse width was made long enough to avoid any spectral diffusion effects, i.e., long enough to saturate the entire line in order that the observed recovery should represent the approach of all the spins within the line to thermal equilibrium, rather than the "spectral diffusion" time for a hole burned in the line to diffuse throughout the line.[48] The relaxation times were measured by comparing the recovering signal with an electronically generated exponential signal. The spin relaxation signal $V_y = V_0 \exp(-t/T_b)$ from the output of the superheterodyne receiver was applied to the vertical input of a Tektronix type 531A oscilloscope; an exponentially varying voltage $V_x = -V_0[1-\exp(-t/T')]$ was applied to the horizontal input immediately following the saturating pulse. By adjusting the time constant T' of the exponentially varying voltage until a straight line $V_y = V_x + V_0$ was observed on the scope, the relaxation time $T_b = T'$ could be determined directly in seconds by reading the calibrated dial on the exponential generator.

The raw data T_b^{-1} versus T were plotted on log-log paper and on semi-log paper to recognize any terms such as T_b^{-1} proportional to T, T^9, or $\exp(-\Delta/kT)$. An equation to best fit the data was found, in some cases by a least-squares program, using an IBM 1620 computer.

In all the experiments except those performed below $T = 1.3$°K, the crystals were immersed in liquid helium which filled the microwave cavity. The experiments below 1.3°K were performed on the apparatus described by Ruby *et al.*,[3] in which the sample is in a vacuum, but

[48] K. D. Bowers and W. B. Mims, Phys. Rev. **115**, 285 (1959); W. B. Mims, K. Nassau, and J. D. McGee, *ibid.* **123**, 2059 (1962).

is thermally bonded to the wall of the cavity, itself a large heat sink. Here the temperature was determined by measuring the resistance of a germanium resistor thermally attached to the microwave cavity. The resistor was obtained from Radiation Research Corporation and was calibrated against the susceptibility of a Curie law salt.[49]

We have measured the velocity of acoustic waves propagating along the [0001] direction in a crystal of LaF_3 which was oriented with x rays and cut into an approximate cube of edge ~ 8 mm with a diamond saw parallel to the (0001), (10$\bar{1}$0), and (11$\bar{2}$0) planes, respectively. Quartz transducers were attached to opposite faces of the crystal with Nonaq stopcock grease as shown in Fig. 8.[50] Phonon pulses at 30 Mc/sec of approximately 1-μsec duration were generated in one transducer and detected in the other. In fact, many reflections within the sample were detected. By observing the time interval between reflections, the velocity of sound was deduced. Using X-cut transducers the velocity of longitudinal waves along the [0001] direction, i.e., the c axis, was found to be $(6.03\pm0.10)\times10^5$ cm/sec. Using Y-cut transducers, the velocity of transverse waves polarized perpendicular to the y direction and propagating along [0001] was found to be $(2.3\pm0.1)\times10^5$ cm/sec.

Shiren[51] has considered a suitable averaging procedure for the velocity of sound for spin-lattice relaxation. Noting that there are twice as many transverse states as longitudinal states in the Debye phonon spectrum, and averaging over all polarization and propagation directions, and assuming only one transverse velocity and one longitudinal velocity one obtains

$$\frac{1}{v^5}=\frac{1}{45}\left(\frac{2}{v_l^5}+\frac{3}{v_t^5}\right). \tag{24}$$

Assuming for LaF_3, the values $v_l=6\times10^5$ cm/sec and $v_t=2.3\times10^5$ cm/sec, we obtain an average sound velocity $v=3.44\times10^5$ cm/sec.

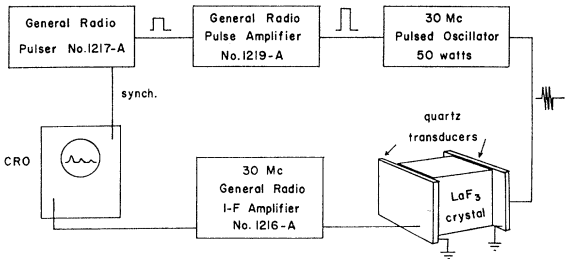

FIG. 8. Block diagram of arrangement for measuring the velocity of sound in LaF_3.

[49] N. C. Ford, Jr., thesis, University of California, 1964 (unpublished); N. C. Ford, Jr., and C. D. Jeffries, Phys. Rev. **141**, 381 (1966).

[50] We are indebted to Dr. R. M. Arzt for the use of his equipment for these measurements.

[51] N. S. Shiren, in *Magnetic and Electric Resonance and Relaxation*, edited by J. Smidt (North-Holland Publishing Company, Amsterdam, 1963), p. 415.

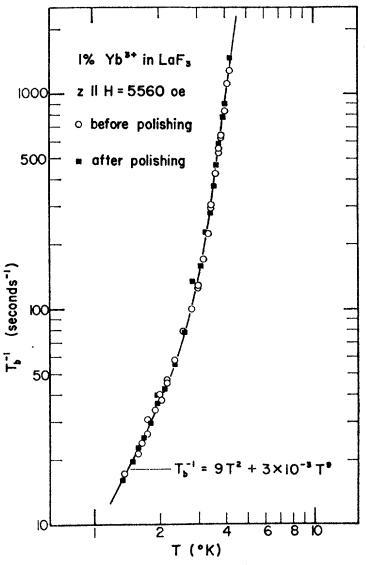

FIG. 9. Observed relaxation rate for 1% Yb^{3+} in LaF_3 with $z\|H$, in the range $1.4<T<5$°K. The rate is essentially unchanged by polishing the crystal.

V. RELAXATION RESULTS AND CALCULATIONS

A. Yb^{3+} in LaF_3

The ground state for Yb^{3+} is $4f^{13}$, $^2F_{7/2}$ which under the action of the LaF_3 crystal field must split into four Kramers doublets. No optical data have yet been reported, so that the energy levels and wavefunctions are not known, and consequently no detailed relaxation calculations can be made.

The magnetic resonance spectrum consists of six main lines plus weak hfs lines due to Yb^{171} and Yb^{173}. Relaxation data were taken on a 1% Yb:LaF_3 crystal at $\nu=9.4$ Gc/sec, $H=5560$ Oe, oriented with the H field parallel to the z axis of one of the magnetic sites, corresponding to $g_z=1.21$. The sample was a rectangular parallelepiped of dimension 0.4 cm$\times$1.15 cm $\times$0.38 cm; it was cut with a 240-grit diamond saw, but not polished. The relaxation data are given in Fig. 9 and have been fitted to the expression

$$T_b^{-1}=9T^2+3\times10^{-3}T^9 \text{ sec}^{-1}. \tag{25}$$

Thinking at first that the T^2 term might be due to a phonon bottleneck, we proceeded to highly polish the faces of the sample with paper impregnated with diamond paste down to 1 micron size; no scratches were visible under 500$\times$ magnification. Relaxation data from the polished sample are also shown on Fig. 9, and do not differ significantly from that of the unpolished sample. This seemed to indicate that if bottlenecked, the phonon lifetime T_{ph} in Eq. (14) is not dependent on surface effects. In phonon bottleneck experiments on soft crystals, S&J found that the phonon lifetime was approximately given by the time of flight of sound through the crystal half-thickness; however efforts to polish the soft crystals so that multiple reflections might occur at the surfaces were not successful. To further

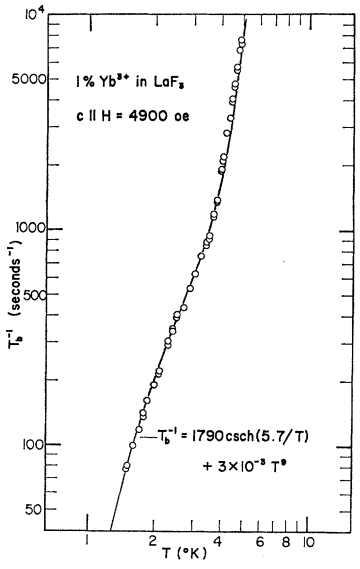

FIG. 10. Observed relaxation rate for 1% Yb^{3+} in LaF_3 with the crystal c axis parallel to H.

investigate the present case of Yb:LaF_3 we sawed from the original boule of Yb:LaF_3 some thin samples of various thicknesses down to 0.25 mm, and measured T_b^{-1} versus T. The relaxation rates were identical to those of Fig. 9, i.e., completely independent of sample size, and seemed to indicate that T_{ph} in Eq. (14) is not the time of flight of sound through the crystal. This leads to two possibilities: either the phonon bottleneck is being broken by an internal process, or else the observed T^2 dependence is not due to a phonon bottleneck. Relaxation data, Fig. 10, were then taken with c parallel to $H=4900$ Oe, where all the six main lines merge; the data are fitted by the expression

$$T_b^{-1}=1790\ \mathrm{csch}(5.7/T)+3\times10^{-3}T^9\ \mathrm{sec}^{-1}. \quad (26)$$

As expected, the Raman term is the same as that of Eq. (25) since it does not depend on magnetic field or orientation according to Eq. (11). However, at the lower temperatures the data are markedly different: the rate is greater where the lines overlap, rather than weaker as would be expected for a phonon bottleneck. Thus we feel that the first term in Eqs. (25) and in (26) is due to cross relaxation, possibly to an excited doublet of a pair of Yb^{3+} ions, as illustrated in Fig. 5, which can lead to an observed relaxation rate with the temperature dependence of Eq. (22) or Eq. (23). The data of Fig. 10 do indeed fit the form of Eq. (22) with $\Delta'=5.7°$K. It can also be fit to Eq. (23) with $\Delta'\approx6°$K, but not as well. This is not an unreasonable value for the exchange energy of a Yb^{3+} pair. Although there appear to be no specific measurements of exchange constants for YbF_3, recent susceptibility measurements[52] on the rare-earth trifluorides indicate that they are mostly antiferromagnetic, with $T_c\sim40°$K for YbF_3. This leads to $\Delta'\sim8°$K if we assume one nearest-neighbor interaction.

Further evidence for the existence of pairs is given by Yen *et al.*[53] who have observed concentration dependent satellite structure in optical studies on the ground state of Er^{3+} in LaF_3. Many satellites are seen with various splittings from the central line up to about 12 cm^{-1}.

It is not surprising that the magnitude and temperature dependence of the cross relaxation terms in Figs. 9 and 10 differ, for the pair energy levels may depend strongly on orientation. For $H\|c$ all nearest-neighbor pairs become equivalent, with an excitation energy $\Delta'\sim6°$K. The T^2 dependence of Fig. 9 may at first be explained by assuming cross relaxation to many different pairs and therefore corresponds to a sum of exponentials as has been observed by Gill[47] for Cr^{3+} in Al_2O_3. However, when the relaxation measurements were extended down to 0.2°K as shown in Fig. 11, the low-temperature region could no longer be fit by a term $T_b^{-1}\propto T^2$. Figure 11 shows data for a crystal of 1% Yb:LaF_3 oriented with the z axis of one of the magnetic sites parallel to H where $\nu=9.5$ Gc/sec, $H=5600$ Oe, and is fitted to

$$T_b^{-1}=6.95[1+\exp(0.47/T)]^{-1}+111\ \mathrm{csch}(3.9/T)+3\times10^{-3}T^9\ \mathrm{sec}^{-1}. \quad (27)$$

The first two terms seem to suggest that cross relaxation is occurring to two distinct types of pairs, the first term being of the form of Eq. (23), i.e., cross relaxation to fast relaxing pairs at $\Delta''=0.47°$; the second term of the form of Eq. (22), for rapid cross relaxation to a different type of pair at $\Delta'=3.9°$K, presumably the

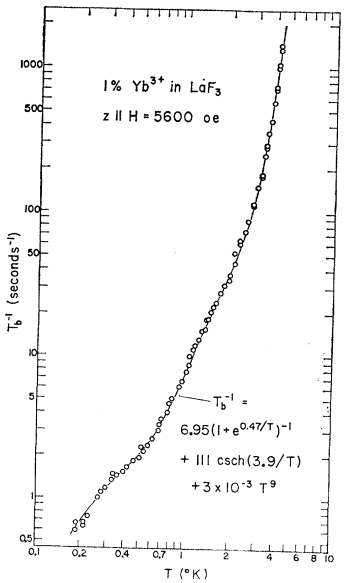

FIG. 11. Observed relaxation rate for 1% Yb^{3+} in LaF_3 with $z\|H$, in the range $0.2<T<5°$K.

[52] S. Kern and P. M. Raccah, J. Phys. Chem. Solids **26**, 1625 (1965).

[53] Y. M. Yen, W. C. Scott, and P. L. Scott, Phys. Rev. **137**, A1109 (1965).

same as for Fig. 10, but with a changed value of Δ' because of the change in orientation. For $0.7<T<2.5$°K, the more strongly coupled system with $\Delta'=3.9$°K is the dominant cross relaxation vehicle; below 0.7°K, these pairs have their excited states sufficiencly depopulated so that now cross relaxation must proceed via the first term, i.e., more weakly coupled pairs, having lower excited states $\Delta''\sim0.47$°K. Apparently, even at 0.2°K, we are unable to see the true direct process in Yb:LaF_3 because of the cross relaxation. However, from Fig. 11 we may estimate that $T_{1d}^{-1}<3T$ sec^{-1} for the true direct process for Yb:LaF_3 at 5600 Oe.

We observed that for certain orientations the paramagnetic resonance lines of Yb:LaF_3 crystals show a superhyperfine[54] structure, as in Fig. 12, which shows the main line (Yb^{172}) and a hyperfine line (Yb^{171}) for the field parallel to the z axis of one of the magnetic sites. Each line is further split into a triplet, but at other orientations much more complicated spectra were observed. We interpret this as due to the overlap of the $4f$ ionic wave function on the fluorine nuclei. Similar structure has been studied by ENDOR and EPR by Ranon and Hyde[54] in Yb^{3+} doped CaF_2. The magnetic resonance work of Lee and Sher[55] on F^{19} in LaF_3 indicate an appreciable covalency in the bonding. Although such superhyperfine structures have been resolved in the paramagnetic resonance spectra of the $5f$ and $6d$ ions, e.g.; U^{3+} in CaF_2,[56] and in the iron group,[54] it is unusual in the $4f$ ions, where the radial extension of the wavefunction is smaller. From the splittings we estimate that the Yb-F hyperfine interaction is of order $A\sim20\times10^{-4}$

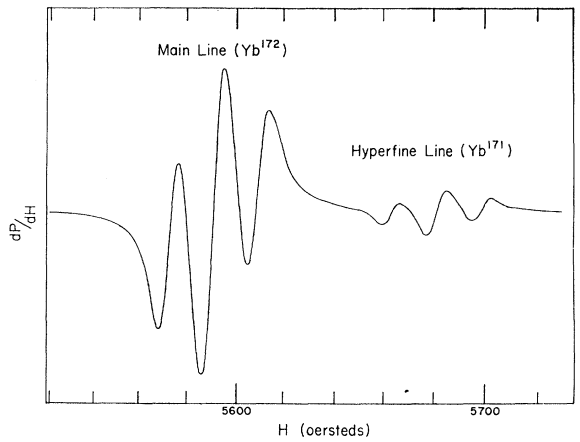

FIG. 12. Part of the paramagnetic resonance spectrum of 1% Yb^{3+} in LaF_3, showing superhyperfine structure. The derivative of the absorption is shown. Both the main line (Yb^{172}) and the hyperfine line (Yb^{171}) are split into a triplet due to hyperfine interaction with the F^{19} nuclei.

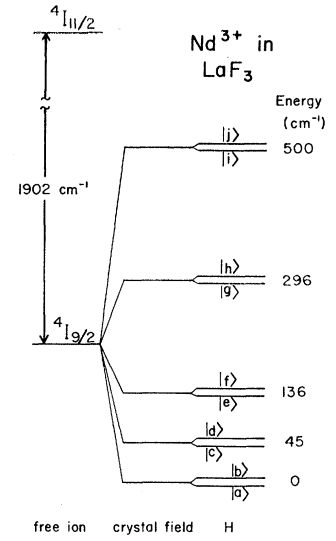

FIG. 13. The $4f^3$, $^4I_{9/2}$ ground multiplet of Nd^{3+} in LaF_3 (Ref. 57).

cm^{-1}. This interaction is unresolved in most of the rare-earth ions in LaF_3, but still accounts for the observed linewidths of 20 to 50 Oe, which are an order of magnitude larger than the Van Vleck dipolar linewidths.

B. Nd^{3+} in LaF_3

The optically determined crystalline field splitting of the $4f^3$, $^4I_{9/2}$ ground multiplet of Nd^{3+} in LaF_3 is shown in Fig. 13 which is constructed from the data of Caspers *et al.*[57] on a $\sim1\%$ Nd:LaF_3 crystal. The crystals were oriented so that the dc magnetic field was parallel to the z axis of the magnetic site whose main line is at 2120 Oe in Fig. 3. All relaxation time measurements were made on this line, corresponding to the g factor $g_z=3.11$.

Relaxation rate data taken at $\nu=9.23$ Gc/sec and $H=2120$ Oe for two samples containing different concentrations of Nd^{3+} are shown in Fig. 14 showing a concentration dependent term $T_b^{-1}\propto T$, a Raman term $\propto T^9$, and a term proportional to $\exp(-\Delta/kT)$. The latter two do not show a significant concentration dependence. A least-squares fitting program which varied the three coefficients of T, T^9, and $\exp(-\Delta/kT)$, and kept $\Delta=65$°K, the value determined from optical measurements[33,57] on Nd^{3+}-doped LaF_3, yielded the results:

$$0.1\%\ \text{Nd},\ T_b^{-1}=0.05\coth(0.22/T)+1.4\times10^{-3}T^9+2.8\times10^{11}\exp(-65/T)\text{sec}^{-1},\quad(28)$$

$$1.0\%\ \text{Nd},\ T_b^{-1}=0.73T+2.4\times10^{-3}T^9+2.4\times10^{11}\exp(-65/T)\text{sec}^{-1}.\quad(29)$$

Since the data for the 0.1% sample was extended to less than 1°K, the exact hyperbolic cotangent function

[54] U. Ranon and J. S. Hyde, Phys. Rev. **141**, 259 (1966), and references therein.

[55] K. Lee and A. Sher, Phys. Rev. Letters **14**, 1027 (1965).

[56] B. Bleaney, P. M. Llewellyn, and D. A. Jones, Proc. Phys. Soc. (London) **69B**, 858 (1956).

[57] H. H. Caspers, H. E. Rast, and R. A. Buchanan, J. Chem. Phys. **42**, 3214 (1965).

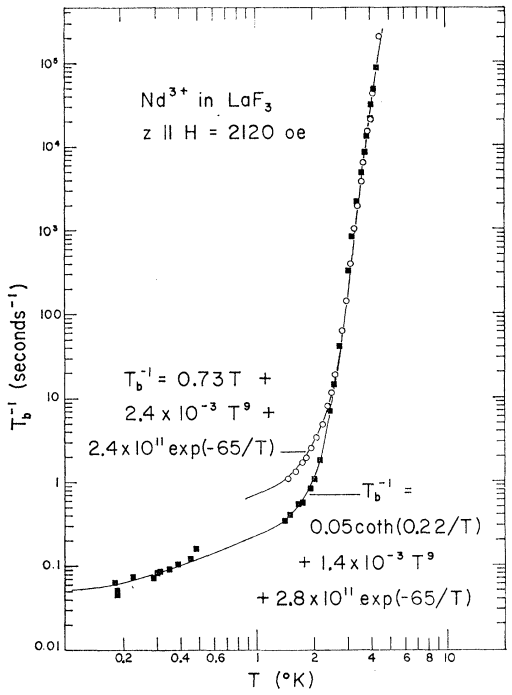

FIG. 14. Relaxation rate T_b^{-1} versus T for two samples of Nd^{3+} in LaF_3 with $z\|H$.

is required to fit the direct process in Eq. (28); this term is approximately $0.23T$ sec^{-1}. The concentration-dependent term linear in T we attribute to cross relaxation to coupled pairs or larger clusters of paramagnetic ions. In some of our more concentrated samples it is possible to see weak extraneous paramagnetic resonance signals which may be due to pairs.

The facts that a factor-of-10 change in concentration changes the relaxation rate by only a factor of 3 at 1.5°K, and because a hyperbolic cotangent dependence of the relaxation rate at low temperatures for the 0.1% Nd sample seems to fit the data, suggests that for this concentration the term linear in T is not far from the true spin-lattice relaxation rate. Relaxation measurements[14] at higher fields and frequencies on this crystal, in fact, show $T_{1d}^{-1} \propto H^4T$ as expected for the direct process.

Using the phenomenological theory reviewed in Sec. III we proceed to a calculation of the relaxation rate for Nd^{3+} in LaF_3 using the static crystal-field parameters and wave functions the calculation of which is outlined in the Appendix. In applying the equations of Sec. III to the calculation of relaxation rates the principal problem is the determination of the dynamic crystal-field parameters a_n^m. We use here two schemes. First, that used by S&J in which certain normalizing factors $g_n^{|m|}$, Table III, are used to estimate the many a_n^m from the optically determined static parameters $A_n^0\langle r^n\rangle$ through the simple relation

$$|a_n^m\langle r^n\rangle| \approx (n+1)g_n^{|m|}|A_n^0\langle r^n\rangle|. \quad (30)$$

TABLE III. Values of the normalizing factors $g_n^{|m|}$ from Ref. 2.

$\|m\|=$	1	2	3	4	5	6
$n=2$	4.90	2.45				
$n=4$	8.95	6.32	23.6	8.37		
$n=6$	12.9	10.2	20.2	11.2	52.7	15.2

And second, we use a scheme defined by

$$|a_n^m\langle r^n\rangle| = (n+1)|A_n^m\langle r^n\rangle|, \text{ even } m \quad (31a)$$

$$|a_n^m\langle r^n\rangle| = \tfrac{1}{2}(n+1)|A_n^{m-1}\langle r^n\rangle + A_n^{m+1}\langle r^n\rangle|, \text{ odd } m. \quad (31b)$$

Although the second scheme seems rather arbitrary, it is simply an empirical attempt to use as fully as possible the known static parameters in selecting suitable average values for the dynamic parameters.

Using the values: crystal density $\rho=6.16$ g/cm^3, effective velocity of sound $v=3.44\times10^5$ cm/sec, $\nu=9.2$ Gc/sec, $H=2120$ Oe, $\Lambda=$Landé g factor$=8/11$ for Nd^{3+}, the data of Fig. 13, we have calculated the direct and Raman rates from Eqs. (8) and (11) using admixtures from all the levels $|a\rangle$, $|b\rangle\cdots|j\rangle$ in the ground multiplet; for the Orbach process Eq. (10) we use levels $|c\rangle$ and $|d\rangle$ and $\Delta=65$°K. The calculation was performed with an IBM 7094 computer using the program of Larson and Jeffries[18] which is fashioned after that of Mikkelson and Stapleton.[19] The results for the scheme of Eq. (30) are

$$1/T_1 = 0.29T + 4.5\times10^{-5}T^9 + 2\times10^{10}\exp(-65/T) \text{ sec}^{-1}. \quad (32)$$

Using the scheme of Eq. (31), we find

$$1/T_1 = 0.29T + 1.6\times10^{-4}T^9 + 1.6\times10^{10}\exp(-65/T) \text{ sec}^{-1}. \quad (33)$$

By the comparison to the data, Eq. (28), we see that the direct process is fairly well estimated, while the Raman and Orbach processes are underestimated by a factor ~10. Although it is typical[18] that the phenomenological approach underestimates the Raman process, it usually does estimate the Orbach process correctly. Accordingly, we refit the data allowing the least-squares fitting program to vary Δ also and ob-obtained a better fit with $\Delta=57$°K for the 0.1% Nd data, yielding an Orbach term $3.6\times10^{10}\exp(-57/T)$ sec^{-1}. We also recalculated Eq. (10) using $\Delta=57$°K to give the theoretical estimates, $1.35\times10^{10}\exp(-57/T)$ and $1.1\times10^{10}\exp(-57/T)$ for the schemes of Eqs. (30) and (31), respectively, which are in far better agreement with the data. A possible reason for this disagreement between values of Δ as observed by our relaxation measurements and those obtained from optical experiments is that for the very dilute sample we used, the energy levels are shifted from the levels for more concentrated samples. For pure NdF_3, $\Delta_1=46$

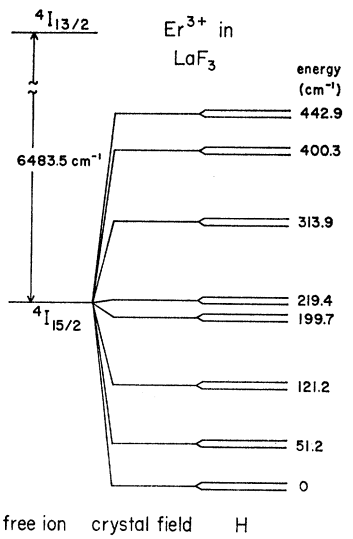

FIG. 15. The $4f^{11}$, $^4I_{15/2}$ ground multiplet of Er^{3+} in LaF_3 (Ref. 59).

cm^{-1} has been reported,[58] while for 1-2% Nd^{3+} in LaF_3 $\Delta_1=44.5-45$ cm^{-1}.[33,57] We also note that similar variations of Δ have been observed in the ethylsulfates[18] and the trichlorides.[20]

C. Er^{3+} in LaF_3

The $4f^{11}$, $^4I_{15/2}$ ground multiplet of Er^{3+} in LaF_3 as determined from optical studies[34,59] is shown in Fig. 15. An orientation with the H field parallel to the x axis of one of the magnetic sites, corresponding to $g_x=2.99$, was chosen for the relaxation measurements in order to best avoid overlap of lines from the other magnetic sites.

Relaxation data taken at $H=2250$ Oe and $\nu=9.3$ Gc/sec over the temperature range $1.3<T<5$°K for five crystals containing different concentrations of Er^{3+} are shown in Fig. 16. For two of the samples the temperature range was extended to $0.2<T<5$°K. The data clearly show a concentration-independent Orbach term $\sim 7.5\times10^{10}\exp(-72/T)$ sec^{-1} and a less well defined Raman term $\sim 2\times10^{-3}\,T^9$ sec^{-1}. However, at all except the highest temperatures there is a strong concentration dependence of the relaxation rate. Accordingly the data at lower temperatures were fitted to terms of the form $\operatorname{csch}(\Delta'/T)$ for the higher concentrations appropriate for cross relaxation; and to terms linear in T or $\coth(\delta/2kT)$ for the lower concentrations, appropriate to the direct process. The data are best fitted by these expressions:

$$0.05\%,\quad T_b^{-1}=0.35\coth(0.22/T)+1.8\times10^{-3}T^9+8.1\times10^{10}\exp(-72/T)\ \text{sec}^{-1},\quad (34)$$

$$0.1\%,\quad T_b^{-1}=24T+6.9\times10^{-4}T^9+7.6\times10^{10}\exp(-72/T)\ \text{sec}^{-1},\quad (35)$$

$$0.2\%,\quad T_b^{-1}=4.6T+1.7\times10^{-3}T^9+7.2\times10^{10}\exp(-72/T)\ \text{sec}^{-1},\quad (36)$$

$$0.5\%,\quad T_b^{-1}=74T+2420\operatorname{csch}(3.9/T)+2\times10^{-3}T^9+7.5\times10^{10}\exp(-72/T)\ \text{sec}^{-1},\quad (37)$$

$$1.0\%,\quad T_b^{-1}=490\operatorname{csch}(3.9/T)+4\times10^{-3}T^9+7.5\times10^{10}\exp(-72/T)\ \text{sec}^{-1}.\quad (38)$$

In Eqs. (35), (36), and (37), the terms in T are concentration-dependent and must not represent the direct process, but, rather, approximations over a limited temperature range to forms like those of Eqs. (23) and (22), the latter being more clearly displayed as the second term in Eq. (37). The value of $\Delta=72$°K agrees well with the optically determined[34,59] value 51 ± 1 cm$^{-1}=73\pm1.4$°K. The Orbach coefficient B for Er^{3+} in LaF_3 has recently been determined by Yen *et al.*[53] from certain optical linewidths to be $B=7.0\pm0.9\times10^{10}$ sec^{-1}, which is in good agreement with the values observed here. Since the observed low-temperature relaxation rates do not appear to be increasing monotonically with concentration, it was thought that the concentrations of the samples were inaccurately known. Therefore, this was checked by orienting each of the five samples exactly alike, placing them in turn in the same position in the microwave cavity and measuring the relative number of spins from the linewidth and intensity of the paramagnetic resonance signals. The results of this showed that the relative concentrations of the five samples marked 0.05, 0.1, 0.2, 0.5, 1% were

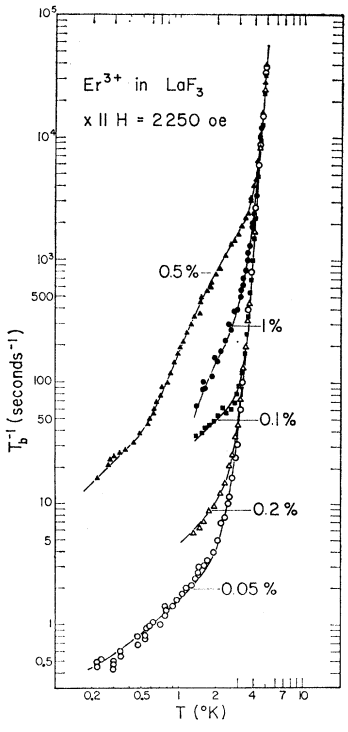

FIG. 16. Relaxation rate T_b^{-1} versus T for five samples of Er^{3+} in LaF_3 with $x\|H$.

[58] Y. K. Chow, Z. Physik **124**, 52 (1947).
[59] W. F. Krupke and J. B. Gruber, J. Chem. Phys. **41**, 1225 (1964).

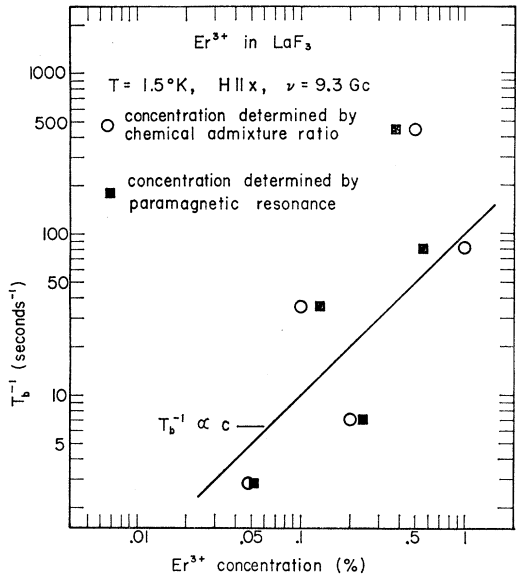

FIG. 17. Concentration dependence of T_b^{-1} at $T=1.5°$K for five samples of Er^{3+} in LaF_3 with $x\|H$.

0.05, 0.13, 0.24, 0.38, 0.55. Figure 17 shows the measured relaxation rates at $T=1.5°$K of the five samples plotted as a function of concentration, unfortunately showing a rather wild scatter of points. Of the many possible *ad hoc* explanations for the concentration dependence one that is certainly possible is that there is an unknown impurity of varying concentration in the samples to which the Er^{3+} can cross relax. Another possibility is that there is cross relaxation to pairs or clusters of Er^{3+} ions, and that there is variable clustering depending on the concentration and the annealing. Although the 0.5% and 1% samples show a temperature and concentration dependence for $1.5<T<3°$K roughly given by $T_b^{-1}\propto T^2/c$ as expected from Eq. (14) for a phonon bottleneck, the following evidence is against this conclusion. First, the condition $AT\gg DT^2$ required for a bottleneck is not met, since values of A from either the theoretical estimates given below or the data at the lowest concentration yield $AT\sim 1$ sec^{-1} to be compared to $DT^2\sim 10^2$ sec^{-1}. Secondly, two thin slabs 0.04 cm and 0.094 cm thick, respectively, of 1% Er:LaF_3 showed the same relaxation rates, whereas the value $D\approx 10^2$ would indicate a mean free path for phonons $\sim$0.25 cm. We also made relaxation measurements at other orientations; a 1% Er:LaF_3 crystal was mounted with the c axis in the horizontal plane, so that the resonance fields for the main lines had the values shown in Fig. 18 as a function of the angle θ between c and the H field. Actually since rotation was about one of the y axes, two pairs of g-tensor axes are equivalent and there are only four main lines instead of six. The relaxation rate T_b^{-1} was measured for the heavy line in Fig. 18 over the angular range $-20°<\theta<+20°$ at $T=1.4°$; only a small variation, $\sim$20%, was observed at $\theta=0$, where all lines merge. If there were a true phonon bottleneck the rate should have decreased sharply as the effective number of spins increased at $\theta=0$. At $\theta=0°$, $H=825$ Oe, T_b^{-1} versus T was measured for $1.4<T<5°$K and the data were best fitted by

$$T_b^{-1}=21T^2+2\times 10^{-3}T^9 +7.5\times 10^{10}\exp(-72/T)\ \text{sec}^{-1}. \quad (39)$$

Finally, when the relaxation measurements were extended to 0.2°K for the 0.5% Er sample, it was found the data could not be fitted by a term $T_b^{-1}\propto\coth^2(\delta/2kT)$ as would be expected for the phonon bottleneck. We feel, therefore, that the concentration dependence of the relaxation rate for all except the very lowest concentration sample is again due to cross relaxation. The experiments on the heavy line of Fig. 18, and further data on $T_b^{-1}(\theta)$ on both Nd:LaF_3 and Er:LaF_3 show that although $T_b^{-1}(\theta)$ may vary by a factor 2 to 10, it usually does not show peaks at values of θ where the different magnetic sites cross. Thus the cross relaxation is likely to excited pairs of Er^{3+} ions or other impurities. Accordingly, the low-temperature data for 0.5% and 1% Er:LaF_3 were fit to a form $T_b^{-1}\propto\text{csch}(\Delta'/T)$ of Eq. (22) as would be expected for strong cross relaxation to excited pairs. As can be seen in Fig. 16 and Eq. (37), the 0.5% data is fit by this form in the range $0.6<T<3°$K, with $\Delta'=3.9°$K. At $T<0.6°$, we have fitted the data by the term $74T$, however. They fit equally well to the term $K[1+\exp(\Delta''/T)]^{-1}$, which, as in the case of Yb above, probably has its origin in cross relaxation to other pairs, cf, Eq. (23). Finally, the low-temperature data on the lowest concentration (0.05%) sample seems to fit a form $T_b^{-1}\propto\coth(\delta/2kT)$ as would be expected for the true direct process. We therefore feel that the direct process is probably revealed in Er:LaF_3 only for concentrations much less than 0.1% and is of order 1 sec^{-1} at 1°K and 2250 Oe.

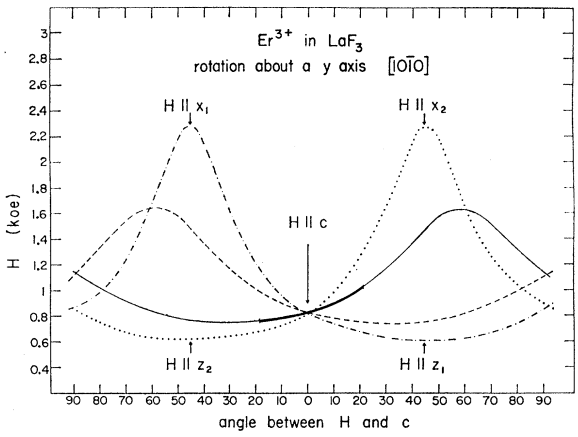

FIG. 18. Observed resonance line positions as a function of angle between the dc magnetic field H and the crystal c axis for a sample of Er^{3+} in LaF_3 at $\nu=9.45$ Gc/sec.

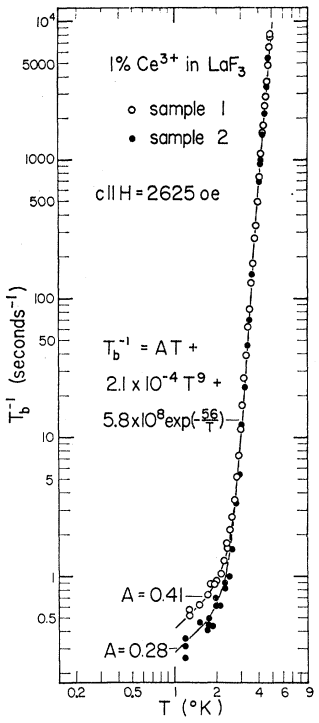

FIG. 19. Observed relaxation rate for two samples of 1% Ce^{3+} in LaF_3, $c\|H$. The difference at low temperature is probably due to a slight concentration difference between the two samples.

We proceed now to an estimate of the relaxation rate by the same procedures as outlined above for Nd^{3+}. The scheme of Eq. (30) gives

$$T_1^{-1}=10T+4.3\times10^{-4}T^9 +1.2\times10^{11}\exp(-72/T)\ \text{sec}^{-1}, \quad (40)$$

and the scheme of Eq. (31) gives

$$T_1^{-1}=0.75T+8.5\times10^{-5}T^9 +1.7\times10^{10}\exp(-72/T)\ \text{sec}^{-1}. \quad (41)$$

The Orbach term in Eq. (40) agrees reasonably well with the observed value, whereas the Raman term is again underestimated somewhat. The agreement also seems moderate for the direct process.

D. Ce^{3+} in LaF_3

Ce^{3+} is the simplest rare earth to treat theoretically, its ground state being $4f^1$, $^2F_{5/2}$. The $^2F_{5/2}$ multiplet is split into three Kramers doublets $|a\rangle$ and $|b\rangle$, $|c\rangle$ and $|d\rangle$, $|e\rangle$ and $|f\rangle$ by the crystal field; the next multiplet[60] $^2F_{7/2}$ being higher by 2253 cm^{-1}; the levels are similar to Fig. 4. Figure 19 shows relaxation data at $\nu=9.3$ Gc/sec, $H=2625$ Oe for two crystals of 1% Ce:LaF_3 oriented with H parallel to the c axis. The data are fitted best by the expressions

$$T_b^{-1}=0.41T+2.1\times10^{-4}T^9 +5.8\times10^{8}\exp(-56/T)\ \text{sec}^{-1}, \quad (42)$$

$$T_b^{-1}=0.28T+2.1\times10^{-4}T^9 +5.8\times10^{8}\exp(-56/T)\ \text{sec}^{-1}. \quad (43)$$

The slight difference in the low-temperature data is undoubtedly due to a slight difference in concentration of the two samples since they came from two different sources. Sample No. 1 came from Hugh Muir of Varian Company whereas sample No. 2 was obtained from Dr. H. H. Caspers, who obtained it from Optovac Company. The exponential term at first suggested an Orbach process via an excited state for Ce^{3+} in LaF_3 at $\Delta_1=56°K=39$ cm^{-1}. However, very careful optical work[61] has failed to reveal any excited state in Ce:LaF_3 at this value, but instead seems to indicate an excited state at 151 cm^{-1}; this would give only a very weak Orbach process. A logical explanation for the observed exponential term is that we are observing cross relaxation to Nd^{3+} impurities. As can be seen from Fig. 14, the Nd^{3+} Orbach rate is roughly 10^2 times faster than the observed exponential term for Ce^{3+}, and as was mentioned in Sec. B, the value of Δ for Nd^{3+} as determined from our relaxation measurements is approximately 57°K. Furthermore, for $c\|H$, the Ce^{3+} and Nd^{3+} resonance lines would be only about 130 G apart at $\nu=9.3$ Gc/sec, and since the linewidths are typically 20–50 G, cross relaxation between Ce^{3+} and Nd^{3+} seems quite likely. Since the observed rate for Ce^{3+} is approximately 10^2 weaker than Nd^{3+}, the results can be explained by assuming a Nd^{3+} impurity of the order 0.01%, within the range of impurities in the La used in growing the crystals. The surprising thing about the data, however, is that the two samples from different sources showed the same exponential term; this could be because the starting material La_2O_3 for the two

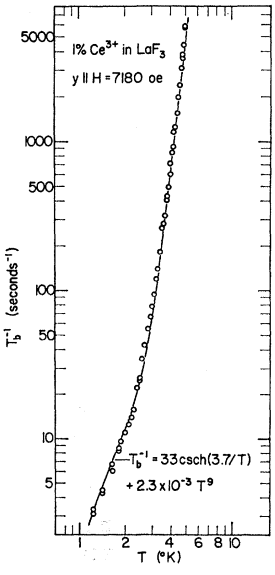

FIG. 20. Observed relaxation rate for 1% Ce^{3+} in LaF_3, $y\|H$.

[60] R. J. Lang, Can. J. Research 14, 127 (1936).

[61] H. H. Caspers (private communication).

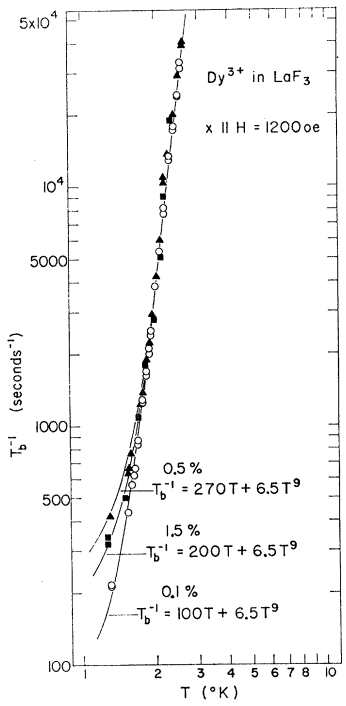

FIG. 21. Observed relaxation rate for three samples of Dy^{3+} in LaF_3, $x\|H$.

crystals had, fortuitously, the same percent of Nd impurity. Further indication that the observed exponential process is not a true Ce^{3+} Orbach process is indicated in Fig. 20, where the relaxation rate versus T of 1% Ce:LaF_3 was measured at another orientation, $y\|H$ = 7180 Oe, and ν = 9.3 Gc/sec. These data are best fitted by

$$T_b^{-1}=33\ \mathrm{csch}(3.7/T)+2.3\times10^{-3}T^9\ \mathrm{sec}^{-1}, \qquad (44)$$

showing no exponential process. The first term seems to indicate that, at low temperatures, for this orientation cross relaxation to excited pairs is now occurring, masking the direct process. Furthermore the T^9 term is an order of magnitude larger than that found for $c\|H$, and possibly represents cross relaxation to another rare earth impurity. In fact, a likely culprit is Dy^{3+}, whose resonance would occur at 7 kOe for $y\|H$, and, as will be seen later, appears to have a very fast Raman process $T_{1R}^{-1}=6.5T^9$.

E. Dy^{3+} in LaF_3

The ground state of Dy^{3+} is $4f^9$, $^6H_{15/2}$. No optical data have been reported, so again the crystal-field splittings and wave functions are not known. From the paramagnetic-resonance spectra, we found these parameters $g_x=5.52\pm0.05$, $g_y=0.96\pm0.01$, $g_z=13.2\pm0.2$, $\theta=16\pm2°$ in some disagreement with Baker and Rubins.[31] Dy^{3+} in LaF_3 displayed anomalously large linewidths when H was parallel to any of the y axes, of the order of several hundred gauss. Relaxation measurements on three different concentrations of Dy:LaF_3 taken for the orientation with the x axis of one of the g tensors parallel to H and for ν = 9.3 Gc/sec and H = 1200 Oe are shown in Fig. 21, and are fitted by

$$0.1\%,\ T_b^{-1}=100T+6.5T^9\ \mathrm{sec}^{-1}, \qquad (45)$$

$$0.5\%,\ T_b^{-1}=270T+6.5T^9\ \mathrm{sec}^{-1}, \qquad (46)$$

$$1.5\%,\ T_b^{-1}=200T+6.5T^9\ \mathrm{sec}^{-1}. \qquad (47)$$

The terms linear in T show a concentration dependence, indicating that we are probably again observing cross relaxation to pairs or clusters. Since the concentration dependence is not uniform, there may be variable clustering occurring, as was seen in Er:LaF_3. The T^9 term, although apparently concentration independent, is three to four orders of magnitude faster than seen in any other LaF_3 crystals containing rare earths and therefore may not be the true Raman process. Furthermore, when relaxation measurements were made for other orientations the data could no longer be fitted to terms of the form $T_b^{-1}\propto T^9$, but instead showed an exponential dependence, as would be expected for an Orbach process. However, this exponential dependence also turned out to be concentration dependent. Because of this orientation and concentration dependence, we we cannot assign the exponential behavior to a true Orbach process but instead must assume cross relaxation again; cf. Eq. (23). The value of Δ' needed to fit the data to the form of Eq. (23) varied between 15 and 30°K, suggesting that Dy^{3+} ions are forming much more

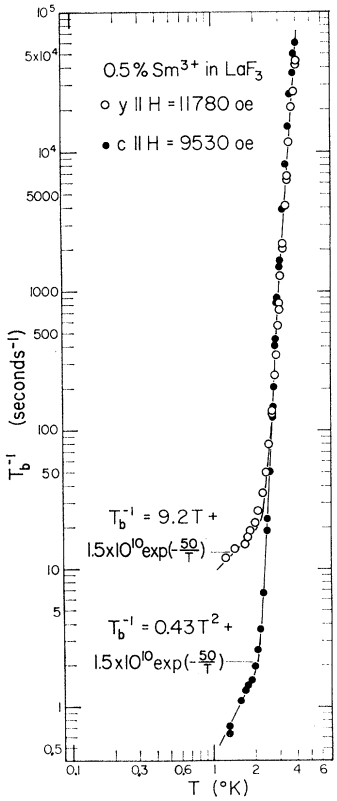

FIG. 22. Observed relaxation rate for 0.5% Sm^{3+} in LaF_3 for $c\|H$ and for $y\|H$.

tightly coupled pairs. To summarize, Dy^{3+} in LaF_3 appears to be a particularly difficult case since the observed relaxation rate is two to three orders of magnitude faster than for other rare earths in LaF_3 and is probably not the true spin-lattice relaxation rate but instead a cross relaxation rate to coupled pairs.

F. Sm^{3+} in LaF_3

The ground state of Sm^{3+} according to Hund's rules is $4f^5$, $^6H_{5/2}$, and in the crystalline field of LaF_3 should split into 3 Kramers doublets. No optical or resonance data has yet been reported for Sm^{3+} in LaF_3. Of all the trivalent rare earths, Sm^{3+} has the smallest Landé g factor, $\Lambda=2/7$. We have observed the paramagnetic resonance from a crystal of 0.5% Sm^{3+} in LaF_3 and find at $T=4.2°K$ and $\nu=9.3$ Gc/sec, the following parameters for Eq. (1):

$$g_x=0.23\pm0.01,\quad g_y=0.558\pm0.005,$$
$$g_z=0.720\pm0.007,\quad \text{and}\quad \theta=(14.5\pm0.2)°.$$

Relaxation data for the two orientations, $y\|H=11780$ Oe and $c\|H=9530$ Oe taken at $\nu=9.2$ Gc/sec are shown in Fig. 22 are fitted by

$$c\|H,\ T_b^{-1}=0.43T^2+1.5\times10^{10}\exp(-50/T)\text{sec}^{-1},\quad (48)$$

$$y\|H,\ T_b^{-1}=9.2T+1.5\times10^{10}\exp(-50/T)\text{sec}^{-1}.\quad (49)$$

The observed Orbach process seems to suggest that the first excited state for Sm:LaF_3 is at approximately 35 cm^{-1}. It is unlikely that this Orbach process is due to cross relaxation as was observed for Ce:LaF_3 because the resonance lines for all the other Kramers ions in LaF_3 would not lie near the Sm^{3+} line since the Sm^{3+} g factors are so small. No Raman process could be detected, indicating that the relaxation rate due to this process is $T_{1R}^{-1}<2\times10^{-3}T^9$. There is a large anisotropy in the relaxation rate at the lower temperatures, which we have fitted to terms in T and T^2,

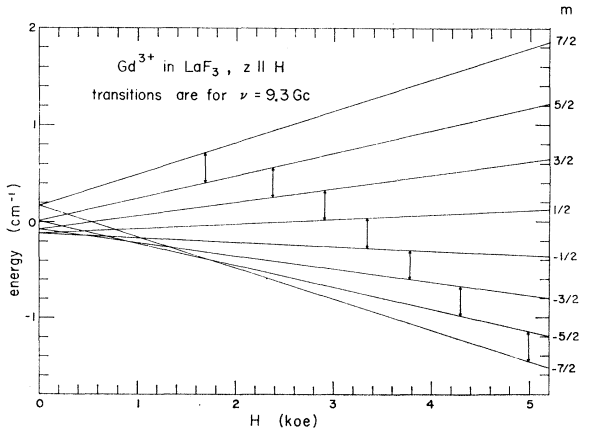

FIG. 23. Energy levels of the $^8S_{7/2}$ ground state of Gd^{3+} in LaF_3 as a function of magnetic field with $H\|z\|c$ axis (see Ref. 30). The $\Delta m=1$ transitions are those observed at 9.3 Gc/sec.

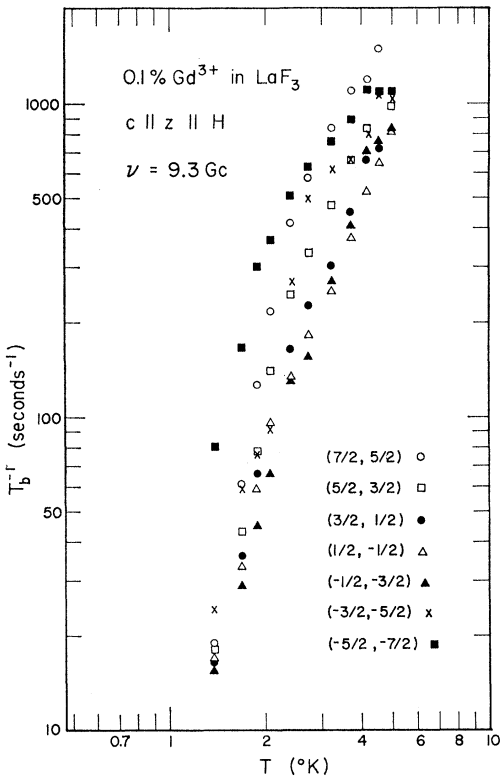

FIG. 24. Relaxation rates observed for the seven $\Delta m=1$ lines of Fig. 23. The relaxation is not exponential and this figure shows the slowest rates observed, near the end of the recovery.

respectively, for the two orientations, $y\|H$, and $c\|H$. However the fact that the concentration dependences was not examined, together with the behavior of the other rare-earth ions above, lead us to suspect that this is neither the true direct process nor a bottleneck, but rather cross relaxation. The temperature range is not wide enough to adequately test the fitting to a form like Eqs. (22) or (23).

G. Gd^{3+} in LaF_3

In first order the ground state of Gd^{3+} is $4f^7$, $^8S_{7/2}$ and should not display any crystal field splitting since the orbital angular momentum is zero. However, because of slight admixtures with excited states due to intermediate coupling there is a small zero field splitting, observed by paramagnetic resonance.[30] This case is thus quite different from the previous ions; Fig. 4 is not a valid representation of the energy levels and the phenomonological relaxation theory in Sec. III is not expected to be valid. Using the Hamiltonian Eq. (2), $S=\frac{7}{2}$, and the parameters of Table II, we show the Zeeman splitting of Gd^{3+} for the c axis parallel to H in Fig. 23. In this case the c axis coincides with the z axes of the g tensors; there are therefore only three inequivalent magnetic sites instead of six. Also shown in Fig. 23 are $\Delta m=1$ resonance transitions for a microwave frequency of

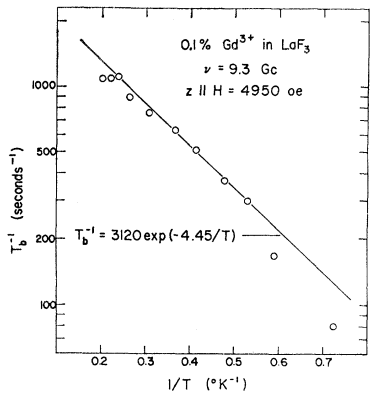

FIG. 25. Relaxation rate versus $1/T$ for the $m=-\frac{7}{2}\rightarrow-\frac{5}{2}$ line of Fig. 23.

$\nu=9.3$ Gc/sec. There are $2S=7$ lines in the paramagnetic resonance spectrum of each site, excluding higher order transitions $\Delta m=2, 3, \cdots$.

At $\nu=9.3$ Gc/sec we have measured the relaxation rate over the temperature range $1.3<T<5$°K for all seven $\Delta m=1$ lines, with the results shown in Fig. 24. In general, the recovery of the Gd^{3+} resonance signal to thermal equilibrium after a saturating pulse was nonexponential, in contrast to the other ions discussed above. The relaxation times recorded were always the longest times observed near the end of the recovery where the signal is just entering the noise. Only for one line, namely, the low field $(\frac{7}{2}\leftrightarrow\frac{5}{2})$ line was a nearly exponential recovery observed. In fact it is theoretically expected that in a multilevel system such as this, the recovery of a disturbed population difference will in general be described by a sum of several exponentials whose time constants are complicated functions of all the relaxation transition probabilities between the various levels.[62] Thus it is difficult to interpret the Gd^{3+} relaxation data other than to say that the over-all temperature dependence $T_b^{-1}(T)$ is in marked contrast to that of the other ions; Fig. 24 shows that T_b^{-1} versus T is steeper at 1.5°K than it is at 4°K. We have taken the data for the $(-\frac{7}{2}\leftrightarrow-\frac{5}{2})$ high-field line and replotted it in Fig. 25, where it is seen that it fits moderately well the form

$$T_b^{-1}=3120\exp(-4.45/T)\text{sec}^{-1}. \quad (50)$$

As the value of $\Delta=4.45$°K is close to the splitting $\Delta'=4.75$°K between the $m=-\frac{5}{2}$ and $m=+\frac{7}{2}$ levels at 5000 Oe, this suggests that the relaxation is via an Orbach type of two phonon process through the higher $m=+\frac{7}{2}$ level in Fig. 23. However, the Orbach process for, say, the low field line $(\frac{7}{2}\leftrightarrow\frac{5}{2})$ should not have this same temperature dependence, whereas the data, Fig. 24, show that all the lines have roughly the same temperature dependence. A Raman process with a temperature dependence $T_{1R}^{-1}\propto T^5$ has been predicted[63] for multilevel systems with $\Delta<kT$; the data show a slope of nearly T^5 at the lowest temperatures, but do not go over to a form T^7 or T^9 at the higher temperatures, as theoretically expected for the Raman process. We note that relaxation data[12] for Gd^{3+} in tetragonal sites in CaF_2 do not at all resemble that of Fig. 20. Finally, the order of magnitude of the relaxation rate seems too large, for Gd^{3+} should be only very weakly coupled to the lattice. To summarize, we cannot yet explain the data as representing spin-lattice relaxation, and so suggest that cross relaxation to pairs or impurities is again playing a significant role.

VI. SUMMARY AND CONCLUSIONS

We have measured the lattice-bath relaxation rate for all the trivalent rare-earth Kramers ions diluted into LaF_3. Although there are six magnetic sites, the lines can be well resolved and the relaxation data are quite reproducable. Except for Gd^{3+}, which behaves differently, the data show the following general features. A Raman process term is often observed, of order $T_{1R}^{-1}\sim10^{-3}\,T^9$ sec^{-1}. For Nd^{3+} and Er^{3+} we observe an exponential Orbach process $\propto\exp(-\Delta/T)$ with $\Delta(Nd)=57$°K, $\Delta(Er)=72$°K, in close agreement with optical data. For Sm^{3+} we also observe an Orbach process with $\Delta=50$°K, but there is no optical data with which to compare this value. Yb^{3+} does not display an Orbach process, indicating that $\Delta>75$°K; Ce^{3+} appears to have a very weak spin-lattice relaxation so is very susceptible to cross relaxation to impurities, probably Nd and Dy, but does not appear to display an Orbach process as would be expected if Δ were greater than ~75°K. Dy^{3+} seems to relax two or three orders of magnitude faster than the other Kramers ions at helium temperatures, possibly via strongly coupled pairs; it also does not display an Orbach process; it is possible that one is being obscured by the cross relaxation. At the lower helium temperatures we observe a term $\propto T$ for Ce^{3+}, Nd^{3+}, Er^{3+}, Dy^{3+} and Sm^{3+}. However this term was found to be concentration dependent in all cases, except Sm^{3+}, where only one concentration was available however. At higher concentrations it took the form T^2 or even $\text{csch}(\Delta'/T)$. We conclude that the true direct process is usually not observed, except possibly for Er and Nd in lowest concentrations, but that cross relaxation to fast relaxing centers, say, pairs of ions, is usually dominant over the direct process. This is in marked contrast to the results on the softer hydrated crystals LaMN and LaES[2,3,18] in which the direct process is relatively strong and easily observable; furthermore, cross relaxation is relatively weak because of the larger atomic spacing of the magnetic ions. On the other hand, in LaF_3 the velocity of sound is about twice greater, so that the direct process may be an order of magnitude weaker; also the atomic spacing between magnetic ions

[62] See, for example, A. E. Siegman, *Microwave Solid-State Masers* (McGraw-Hill Book Company, Inc., New York, 1964), p. 171 ff; J. P. Lloyd and G. E. Pake, Phys. Rev. **94**, 579 (1954); W. J. C. Grant, J. Phys. Chem. Solids **25**, 751 (1964).

[63] R. Orbach and M. Blume, Phys. Rev. Letters **8**, 478 (1962).

TABLE IV. Summary of measured relaxation rates (in sec^{-1}) at helium temperatures, theoretical estimates, and M^2 defined by Eq. (51) for some rare-earth ions diluted in single crystals of LaF_3.

Ion	Conc.	Orientation	Quantity	Relaxation Rate (in sec^{-1}) and M^2 corresponding to each term	Δ
Ce^{3+}	1.0% No. 1	$c\|\|H=2625$ Oe	meas. Eq. (42)	$0.41T+5.8\times10^{8}\exp(-56/T)+2.1\times10^{-4}T^{9}$	217°K[a]
	1.0% No. 2	$c\|\|H=2625$ Oe	meas. Eq. (43)	$0.28T+5.8\times10^{8}\exp(-56/T)+2.1\times10^{-4}T^{9}$	
			M^2:	12 35	
	1.0% No. 1	$y\|\|H=7180$ Oe	meas. Eq. (44)	$33\,\mathrm{csch}(3.7/T)+2.3\times10^{-3}T^{9}$	
Nd^{3+}	0.1%	$z\|\|H=2120$ Oe	meas. Eq. (28)	$0.23T+2.8\times10^{11}\exp(-65/T)+1.4\times10^{-3}T^{9}$	65°K[b]
			M^2:	21 380 86	
			theor. Eq. (33)	$0.29T+1.6\times10^{10}\exp(-65/T)+1.6\times10^{-4}T^{9}$	
			meas.[c]	$0.23T+3.6\times10^{10}\exp(-57/T)+10^{-3}T^{9}$	57°K[c]
			M^2:	*21 88 76*	
			theor.[c]	$0.38T+1.1\times10^{10}\exp(-57/T)+2.7\times10^{-4}T^{9}$	
	1.0%	$z\|\|H=2120$ Oe	meas. Eq. (29)	$0.73T+2.4\times10^{11}\exp(-65/T)+2.4\times10^{-3}T^{9}$	65°K
Sm^{3+}	0.5%	$c\|\|H=9530$ Oe	meas. Eq. (48)	$0.43T^{2}+1.5\times10^{10}\exp(-50/T)$	50°K[d]
		$y\|\|H=11\,780$ Oe	meas. Eq. (49)	$9.2T+1.5\times10^{10}\exp(-50/T)$	
			M^2:	170 *72*	
Gd^{3+}	0.1%	$c\|\|H=4950$ Oe	meas.[e] Eq. (50)	$3120\exp(-4.45/T)$	
Dy^{3+}	0.1%	$x\|\|H=1200$ Oe	meas. Eq. (45)	$100T+6.5T^{9}$	unknown
			M^2:	8300 6100	
	0.5%	$x\|\|H=1200$ Oe	meas. Eq. (46)	$270T+6.5T^{9}$	
	1.5%	$x\|\|H=1200$ Oe	meas. Eq. (47)	$200T+6.5T^{9}$	
Er^{3+}	0.05%	$x\|\|H=2250$ Oe	meas. Eq. (34)	$1.6T+8.1\times10^{10}\exp(-72/T)+1.8\times10^{-3}T^{9}$	72°K
			M^2:	*47 65 100*	
			theor. Eq. (40)	$10T+1.2\times10^{11}\exp(-72/T)+4.3\times10^{-4}T^{9}$	
	0.1%	$x\|\|H=2250$ Oe	meas. Eq. (35)	$24T+7.6\times10^{10}\exp(-72/T)+6.9\times10^{-4}T^{9}$	
	0.2%	$x\|\|H=2250$ Oe	meas. Eq. (36)	$4.6T+7.2\times10^{10}\exp(-72/T)+1.7\times10^{-3}T^{9}$	
	0.5%	$x\|\|H=2250$ Oe	meas. Eq. (37)	$74T+2420\,\mathrm{csch}(3.9/T)+7.5\times10^{10}\exp(-72/T)+2\times10^{-3}T^{9}$	
	1.0%	$x\|\|H=2250$ Oe	meas. Eq. (38)	$490\,\mathrm{csch}(3.9/T)+7.5\times10^{10}\exp(-72/T)+4\times10^{-3}T^{9}$	
	1.0%	$c\|\|H=825$ Oe	meas. Eq. (39)	$21T^{2}+7.5\times10^{10}\exp(-72/T)+2\times10^{-3}T^{9}$	
Yb^{3+}	1.0%	$z\|\|H=5560$ Oe	meas. Eq. (25)	$9T^{2}+3\times10^{-3}T^{9}$	unknown
			M^2	*130*	
		$c\|\|H=4900$ Oe	meas. Eq. (26)	$1790\,\mathrm{csch}(5.7/T)+3\times10^{-3}T^{9}$	
		$z\|\|H=5600$ Oe	meas. Eq. (27)	$6.95[1+\exp(0.47/T)]^{-1}+111\,\mathrm{csch}(3.9/T)+3\times10^{-3}T^{9}$	

[a] Reference 61.
[b] References 33 and 57.
[c] Δ = 57°K determined from best fit to relaxation data for 0.1% Nd:LaF_3.
[d] Δ = 50°K determined from best fit to relaxation data.
[e] High field $\Delta m=-7/2\rightarrow-5/2$ line only.

is closer by a factor of two, and there is evidence of superhyperfine interaction with the F nuclei, all of which will make a pair of ions more tightly coupled to the lattice, hence a source of cross relaxation to single ions, which can mask the true direct process. A similar behavior is found for rare earth ions in CaF_2[12] and garnets[17] probably for the same reasons.

For the relatively high concentrations of 1% Er^{3+} and Yb^{3+}, and 0.5% Sm^{3+}, the data showed a temperature dependence $T_b^{-1}\propto T^2$ for temperatures higher than 1.3°K. However, this was found to be independent of crystal size or surface polish, but orientation dependent. Since the direct process is weak, this is very likely not a phonon bottleneck but rather, cross relaxation. We attribute the apparent T^2 dependence as an approximation to the form $\mathrm{csch}(\Delta'/T)$, expected for cross relaxation to an excited doublet at Δ′. In fact this dependence was clearly observed for Yb^{3+} and Er^{3+} at lower temperatures, down to 0.2°K. The value of Δ′ is found to lie between 4 and 6°K, and suggests cross relaxation to an excited doublet of a pair of Yb^{3+} or Er^{3+} ions. These values of Δ′ are not unreasonable when compared with estimates based on the exchange coupling in the trifluorides.

The over-all experimental results are summarized in Table IV. Only for Nd^{3+} and Er^{3+} are we able to theoretically estimate the relaxation rates from wave functions and static crystal-field parameters, since the pertinent optical data are lacking in the other cases. We have made theoretical estimates from the simple phenonenological model of Sec. III, and list the results for Nd^{3+} and Er^{3+} in Table IV, along with the data. For the Orbach term, there is reasonable agreement with the experimental value for Er^{3+}; for Nd^{3+} the theory underestimates this process by ~10 using the optical value Δ = 65°K, but the data fit better for Δ = 57°K and this value in the theory does yield a reasonable agreement. The theory consistently underestimates the Raman process by an order of magnitude. Since the Raman process depends in detail on the phonon spectrum, this

may indicate that the assumption $\rho(\nu) \propto \nu^2$ is simply not a very good approximation. The calculated direct process is in reasonable agreement with the low-temperature relaxation rate data for the lowest concentrations of Nd^{3+} and Er^{3+}.

To make a further, statistical, analysis of the data of Table IV, we have inverted the problem and calculated the quantity.

$$M^2 \equiv \sum_{n,m,i} \frac{|\langle a|v_n{}^m|i\rangle|^2}{\Delta_i{}^2} \tag{51}$$

required to explain the observed direct and Raman processes by Eqs. (8) and (11), respectively. In so doing we have made the approximations $|\langle a|v_n{}^m|i\rangle| \approx |\langle i|v_n{}^m|b\rangle|$ and $\langle a|\mathbf{H}\cdot\mathbf{J}|i\rangle \approx H$. We calculate a similar quantity, but without the sum over i, to explain the Orbach rate by Eq. (10), thus taking matrix elements only to the first excited state at $\Delta=\Delta_1$; this, however, should be comparable to Eq. (51), since the first state usually contributes most significantly. These values of M^2 are listed in Table IV immediately below the observed rate from which they are derived. Since some of the observed rates probably do not represent true spin-lattice relaxation, as discussed above, we have italicized and used below only those values of M^2 which are thought to derive from true spin-lattice relaxation; the values range from 21 to 130. In order to compare these we calculate $M^2\Delta_1{}^2$, which should represent approximately $\sum_{n,m}|\langle a|v_n{}^m|c\rangle|^2$, which should not vary greatly for the various rare-earth ions in LaF_3. The values of $M^2\Delta_1{}^2$ range from 0.3×10^5 to 2.5×10^5 cm^{-2}, the average being 1.2×10^5 cm^{-2}, which we take as a representative value, useful in estimating other relaxation rates. For example, we would estimate for $Ce:LaF_3$ using $\Delta_1=151$ cm^{-1},[61] that $T_1{}^{-1}\approx 0.1T+3\times10^{-5}T^9$ sec^{-1}, indicating that the observed rates, Eqs. (42) and (43), are probably limited by cross relaxation. Similarly, one can speculate that the observed rates for $Dy:LaF_3$ are orders faster than one estimates, unless Δ_1 is as small as ~10 cm^{-1}, in which case the failure to observe an Orbach process is not understood.

To summarize, in Table IV the observed rates are very likely the true spin lattice relaxation rates for the direct process for Nd and Er; the Orbach process for Nd, Sm, and Er; and the Raman process for Nd, Er, Yb.

ACKNOWLEDGMENTS

Thanks are due to Dr. P. L. Scott and Dr. W. M. Yen and Hugh Muir for samples, to Dr. H. J. Stapleton and Dr. R. C. Mikkelson for the use of their computer program, to J. M. McColl for much help with computer programming, and to Dr. E. A. Harris, Dr. G. H. Larson, K. S. Yngvesson, T. E. Gunter, and K. H. Langley for many stimulating and enlightening discussions.

APPENDIX

In order to make estimates of the spin-lattice relaxation rate using the theory of Sec. III, it is necessary to know the static crystal-field parameters $A_n{}^m\langle r^n\rangle$ in Eqs. (30) and (31). Using a Newton-Raphson[64] least-squares fitting method and an IBM 7094 computer we have attempted to find values for $A_n{}^m\langle r^n\rangle$ which best yield the optically determined energy levels and spin-resonance-determined ground-doublet g factors for Nd^{3+} and Er^{3+} in LaF_3. For Nd^{3+}, the entire 26×26 crystal field and LS coupling matrix describing all the ^4I levels was diagonalized using for the crystal field, reduced matrix elements appropriate to intermediate coupling.[65] For Er^{3+} only the 8×8 crystal field matrix for the $^4I_{15/2}$ multiplet was diagonalized without considering intermediate coupling, spin-orbit coupling or crystal field admixtures to higher multiplets.

Because the theory of Sec. III gives only an order of magnitude estimate of the spin-lattice relaxation rate and because of the discrepancy of the La site symmetry in LaF_3, it was decided to make the problem simpler by assuming the site symmetry at the La ion to be C_{2v}, which requires only nine parameters. Actually, the symmetry is C_2 or C_s requiring 15 parameters. Attempts to find a unique set of crystal field parameters and wave functions which explained the energy levels were not successful; the results depend on the starting values and no unique convergence was obtained. This is probably because the ordering of the levels is not known *a priori*. This procedure thus yields only rough magnitudes of the $A_n{}^m\langle r^n\rangle$, varying from 20 to 900 cm^{-1}. Next we put in the additional input data, the ground-stage g factors. This did not really yield a unique fit either and so we used in the calculations in Sec. V a representative set of parameters, of order 150 cm^{-1} and a representative set of wave functions. This is indeed a rough approximation, but then so is the procedure in Sec. III for the calculation of the relaxation rates. However, the large number of parameters gives a statistical nature to the problem which is the only justification for these procedures.

[64] See, for example, J. B. Scarborough, *Numerical Mathematical Analysis* (Oxford University Press, New York, 1950), p. 192ff.
[65] B. G. Wybourne, J. Chem. Phys. 34, 279 (1961).